# Size-dependent behaviour of functionally graded sandwich microplates under mechanical and thermal loads

Luan C. Trinh [a,b], Thuc P. Vo [a,*], Huu-Tai Thai [c], JL Mantari [d]

[a] Department of Mechanical and Construction Engineering, Northumbria University, Ellison Place, Newcastle upon Tyne NE1 8ST, UK

[b] Faculty of Civil Engineering, Ho Chi Minh City University of Technology and Education, 1 Vo Van Ngan Street, Thu Duc District, Ho Chi Minh City, Vietnam.

[c] School of Engineering and Mathematical Sciences, La Trobe University, Bundoora, VIC 3086, Australia

[d] Faculty of Mechanical Engineering, Universidad de Ingeniería y Tecnología, Jr. Medrano Silva 165, Barranco, Lima, Perú

**Abstract**

This paper presents the static bending, free vibration and buckling behaviours of functionally graded sandwich microplates under mechanical and thermal loads. Governing equations of both higher-order shear deformation and quasi-3D theories are derived based on the variational principle and modified couple stress theory. Apart from mechanical load, the temperature profiles considered are either uniform or linear distribution through the thickness, which results in changes of material properties and stress resultants. Numerical results are obtained using Navier solutions. The difference between quasi-3D and 2D models in dealing with mechanical and thermal load is discussed. Temperature-dependent and temperature-independent material properties are examined. The effects of geometry and power-law index together with mechanical loads and various temperature distributions on the size-dependent behaviours of functionally graded sandwich plates are also investigated.

*Keywords*: Functionally graded plate, sandwich plate, modified couple stress theory, quasi-3D theory.

[*] Corresponding author. Tel.: +44 (0) 191 243 7856

E-mail address: luanc.trinh@gmail.com (Luan C. Trinh); thuc.vo@northumbria.ac.uk (Thuc P. Vo).

## 1. Introduction

Functionally graded materials (FGMs) are a kind of composite materials in which the material components are the mixture of two or more constituents. By gradually changing the volume fraction of materials, the desirable material properties can be tailored continuously, and thus avoiding the delamination phenomenon occurred in laminated composites. In addition, being usually manufactured by metal and ceramic components, which are qualified for superior strength and thermal insulation, functionally graded (FG) structures possess striking features for engineering applications. The use of FGMs becomes more promising when they are combined with sandwich structures to create FG sandwich structures. In such structures, a FG layer is usually sandwiched between homogeneous skins to form FG core-homogeneous skins sandwich; otherwise, a homogeneous core is inserted to two FG layers to create homogeneous core- FG skins sandwich. By this way, the structures can be customised with thicker skins or symmetric configurations.

Applications of small-scale structures inspire new research on the behaviours of micro/nano structures. There are three main methods to analyse such small-scale structures including molecular dynamics simulation, hybrid molecular-continuum methods, and non-classical continuum methods [1]. Among them, the third one is computationally effective and thus widely applicable to solid structures. The development of these micro-continuum methods can be outlined from the introduction of the additional degrees of freedom of rotation at each material particle in Cosserat continua [2] by introducing material length scale parameters. Insightful discussions about classical couple stress theories [3-6] and other non-classical continuum theories including strain gradient [3, 4], modified strain gradient [5], nonlocal elasticity [6] and modified nonlocal elasticity [7-11] can be found in [5, 10, 12-14]. The main challenge of these theories is how to determine correctly material length scale parameters. The Modified Couple Stress Theory (MCST) has advantages over other size-dependent theories since it has only one material length scale parameter and includes symmetric couple stress. It is the reason why this theory is widely used in practice. Following is the brief review of the MCST which was developed based on the classical plate theory (CPT), first-order shear deformation theory (FSDT) and higher-order shear deformation theory (HSDT). It should be noted that CPT model is only appropriate for thin plates due to neglecting shear deformation effect. Based on this model, Ke et al. [15] investigated the static bending, free vibration and buckling behaviours of FG annular microplates with various boundary conditions (BCs). The formulations for arbitrary shape and free vibration of FG rectangular microplates was examined by Asghari and Taati [16]. Geometric nonlinearity was accounted for in Taati's work [17] for buckling and post-buckling behaviours of FG microplates under different BCs using analytical solutions. To overcome the limitation of the CPT model, FSDT model has been proposed by assuming the in-plane displacements vary linearly through the thickness. Thus, a shear correction factor is necessary. Using this model, analytical solutions were developed to linear and nonlinear bending, vibration and buckling analysis of simply supported FG microplates by Thai and Choi [18]. Jung et al. [19, 20] included the elastic foundation in the behaviour of FG microplates. Ansari et al. [21, 22] also developed a nonlinear model for the vibration, bending and post-buckling analysis of FG microplates. In order to eliminate the use of the shear correction factor and obtain a better prediction of responses for thick plates, several HSDTs have been proposed. These models were applied to investigate bending and free vibration behaviours of FG microplates by Thai and Kim [23] using analytical solutions and annular/circular microplates by Eshraghi [24] using the differential quadrature (DQ) method. Thai and Vo [25] developed a MCST sinusoidal theory for FG microplates and derived analytical solutions for deflections and natural frequencies of simply supported microplates. He et al. [26] presented a MCST four-variable refined plate model using analytical solution for the FG microplates. Lou et al. [27] then developed this model for a unified framework including the von Karman's geometric nonlinearity. It should be noted that above studies [26-30], the normal strain or normal deformation, which becomes significant for thick plates, is not included. In order to take into account both shear and normal deformation effects, Nguyen et al. [28] presented four-variable quasi-3D model to analyse the bending, vibration and buckling behaviours of FG microplates using the isogeometric solutions.

Thermal effect also has been analysed for FG micro structures in some publications. Reddy and Kim [29] developed theoretical formulation for mechanical and thermal analysis with a general nonlinear model containing cubic and quadratic variations of the in-plane and transverse displacements for FG microplates. They also derived the linear analytical solutions of bending, vibration and buckling behaviours for this model under mechanical loads [30]. Mirsalehi et al. [31] investigated the stability of thin FG microplates under mechanical and thermal loads using CPT based on the spline finite strip method. Using CPT, Ashoori and Vanini [32] also studied thermal buckling of annular FG microplates resting on an elastic medium accounting for geometrically nonlinear effect and snap-through behaviour. Utilising the DQ method, Eshaghi et al. [33] analysed static bending and free vibration responses of FG annular/circular plates based on CPT, FSDT and HSDT models.

Based on the MCST, this paper presents the quasi-3D models, which include both shear and stretching effects, for the bending, vibration and buckling behaviours of FG sandwich microplates under mechanical and thermal loads. The refined plate model, which is obtained by degenerating the thickness stretching effect, is applied to figure out the difference between the 2D and quasi-3D solutions. The unified temperature profile is applied to describe the uniform and linear distribution through the thickness. The effects of geometry and power-law index together with mechanical loads and various temperature distributions on the size-dependent behaviours of FG sandwich microplates are also investigated.

## 2. Theoretical formulation

### 2.1. Functionally graded sandwich plate and temperature-dependent material properties

In this paper, FG plate and two types of FG sandwich plates are considered. The material properties including Young's modulus $E(z)$, thermal expansion coefficients $\alpha(z)$ and mass density $\rho(z)$ are expressed using the rule of mixture:

$$P(z,T)=\left[P_c(z,T)-P_m(z,T)\right]V_c(z)+P_m(z,T) \tag{1}$$

where $P(z)$ is either $E(z)$, $\alpha(z)$ or $\rho(z)$; $c$ and $m$ indicate ceramic and metal. Material properties in the temperature-dependent analysis are calculated for ceramic and metal as [34]:

$$P(T)=P_0\left(P_{-1}T^{-1}+1+P_1T+P_2T^2+P_3T^3\right) \tag{2}$$

where $P_{-1},P_1,P_2$ and $P_3$, given in Table 2, are the temperature-dependent coefficients. To simplify the numerical calculation, Poisson's ratio is measured at the middle-plane's temperature for both metal and ceramic.

The volume fraction of ceramic is described by the power law as below:

*a. FG plate:*

$$V_c(z)=\left(\frac{z}{h}+\frac{1}{2}\right)^p \tag{3a}$$

*b. Sandwich plate with FG core – homogeneous skins:*

$$V_c(z)=\begin{cases}0 & \text{if } z\in[h_0,h_1]\\ \left(\dfrac{z-h_1}{h_2-h_1}\right)^p & \text{if } z\in[h_1,h_2]\\ 1 & \text{if } z\in[h_2,h_3]\end{cases} \tag{3b}$$

*c. Sandwich plate with ceramic core – FG skins:*

$$V_c(z)=\begin{cases}\left(\dfrac{z-h_0}{h_1-h_0}\right)^p & \text{if } z\in[h_0,h_1]\\ 1 & \text{if } z\in[h_1,h_2]\\ \left(\dfrac{z-h_3}{h_2-h_3}\right)^p & \text{if } z\in[h_2,h_3]\end{cases} \tag{3c}$$

*d. Sandwich plate with metal core – FG skins:*

$$V_c(z)=\begin{cases} 1-\left(\dfrac{z-h_0}{h_1-h_0}\right)^p & \text{if } z\in[h_0,h_1] \\ 0 & \text{if } z\in[h_1,h_2] \\ 1-\left(\dfrac{z-h_3}{h_2-h_3}\right)^p & \text{if } z\in[h_2,h_3] \end{cases} \tag{3d}$$

where $p$ is the power law index.

Here, uniform and linear temperatures through the thickness is considered and described by:

$$T(x,y,z)=300+\Delta T_1(x,y)+\frac{z}{h}\Delta T_2(x,y) \tag{4}$$

where $\Delta T_1$ and $\Delta T_2$ determine the uniform increase and the gradient of temperature through the thickness, respectively. In this paper, unless otherwise stated, $\Delta T_2=100K$ which leads to $100K$ higher temperature at the top surface compared to the bottom one.

## 2.2. Kinematics and constitutive relations

Consider a FG sandwich plate with the coordinate and cross-section shown in Fig. 1. By applying the modified couple stress theory, the variation of strain energy is related to both strain and curvature tensors as [12]:

$$\delta\Pi=\int_V(\boldsymbol{\sigma}\delta\boldsymbol{\varepsilon}+\mathbf{m}\delta\boldsymbol{\chi})dV \tag{5}$$

where $\boldsymbol{\varepsilon}$ and $\boldsymbol{\chi}$ are the strain and symmetric curvature tensor defined by:

$$\boldsymbol{\varepsilon}=\frac{1}{2}\left(\nabla\mathbf{u}+(\nabla\mathbf{u})^T\right) \tag{6a}$$

$$\boldsymbol{\chi}=\frac{1}{2}\left(\nabla\boldsymbol{\theta}+(\nabla\boldsymbol{\theta})^T\right) \tag{6b}$$

$\boldsymbol{\sigma}$ and $\mathbf{m}$ are the corresponding stress and deviatoric part of the symmetric couple stress tensors defined by:

$$\boldsymbol{\sigma}=\lambda tr(\boldsymbol{\varepsilon})\mathbf{I}+2\mu\boldsymbol{\varepsilon} \tag{7a}$$

$$\mathbf{m}=2l^2\mu\boldsymbol{\chi} \tag{7b}$$

in which, $\lambda=\dfrac{E\nu}{(1+\nu)(1-2\nu)}$ and $\mu=\dfrac{E}{2(1+\nu)}$ are Lame's constants, $l$ is the material length scale parameter [12], $\mathbf{u}=(u_1,u_2,u_3)$ and $\boldsymbol{\theta}=(\theta_x,\theta_y,\theta_z)$ are the displacement and rotation vectors expressed below.

The displacement field which includes the normal stretching effect is assumed to an arbitrary point as:

$$u_1(x,y,z,t)=U(x,y,t)-z\frac{\partial W_b(x,y,t)}{\partial x}-f(z)\frac{\partial W_s(x,y,t)}{\partial x} \tag{8a}$$

$$u_2(x,y,z,t)=V(x,y,t)-z\frac{\partial W_b(x,y,t)}{\partial y}-f(z)\frac{\partial W_s(x,y,t)}{\partial y} \tag{8b}$$

$$u_3(x,y,z,t)=W_b(x,y,t)+W_s(x,y,t)+g(z)W_z(x,y,t) \tag{8c}$$

where $U$ and $V$ are in-plane displacements, $W_b,W_s$ and $W_z$ are bending, shear and stretching displacements of a point on the middle plane. $f(z)$ and $g(z)=1-\frac{df(z)}{dz}$ are the shape functions which distribute the effect of $W_s$ and $W_z$ across the thickness. Two sets of shape functions are applied [35-37]:

Third-order shear deformation theory (TSDT): $f(z)=\frac{4}{3}\frac{z^3}{h^2}$ (9a)

Sinusoidal shear deformation theory (SSDT): $f(z)=z-\frac{h}{\pi}sin\frac{\pi z}{h}$ (9b)

The rotation vector is expressed as:

$$\boldsymbol{\theta}=\frac{1}{2}curl\,\mathbf{u}=\frac{1}{2}\left[\left(\frac{\partial \mathrm{u}_3}{\partial y}-\frac{\partial \mathrm{u}_2}{\partial z}\right)\mathbf{e_x}+\left(\frac{\partial \mathrm{u}_1}{\partial z}-\frac{\partial \mathrm{u}_3}{\partial x}\right)\mathbf{e_y}+\left(\frac{\partial \mathrm{u}_2}{\partial x}-\frac{\partial \mathrm{u}_1}{\partial y}\right)\mathbf{e_z}\right] \tag{10a}$$

$$\theta_x=\frac{1}{2}curl\,u\Big|_{\mathbf{e_x}}=\frac{\partial W_b}{\partial y}+\frac{1}{2}\left(1+\frac{\partial f(z)}{\partial z}\right)\frac{\partial W_s}{\partial y}+\frac{1}{2}g(z)\frac{\partial W_z}{\partial y} \tag{10b}$$

$$\theta_y=\frac{1}{2}curl\,u\Big|_{\mathbf{e_y}}=-\frac{\partial W_b}{\partial x}-\frac{1}{2}\left(1+\frac{\partial f(z)}{\partial z}\right)\frac{\partial W_s}{\partial x}-\frac{1}{2}g(z)\frac{\partial W_z}{\partial x} \tag{10c}$$

$$\theta_z=\frac{1}{2}curl\,u\Big|_{\mathbf{e_z}}=\frac{1}{2}\left(\frac{\partial \mathrm{V}}{\partial x}-\frac{\partial \mathrm{U}}{\partial y}\right) \tag{10d}$$

The strain components related to above displacement field are presented by substituting Eq. (8) to Eq. (6a):

$$\varepsilon_{xx}=\frac{\partial U}{\partial x}-z\frac{\partial^2 W_b}{\partial x^2}-f(z)\frac{\partial^2 W_s}{\partial x^2}-\alpha(z,T)\Delta T(x,y,z) \tag{11a}$$

$$\varepsilon_{yy}=\frac{\partial V}{\partial y}-z\frac{\partial^2 W_b}{\partial y^2}-f(z)\frac{\partial^2 W_s}{\partial y^2}-\alpha(z,T)\Delta T(x,y,z) \tag{11b}$$

$$\varepsilon_{zz}=\frac{\partial g(z)}{\partial z}W_z-\alpha(z,T)\Delta T(x,y,z) \tag{11c}$$

$$\gamma_{xy} = 2\varepsilon_{xy} = \frac{\partial U}{\partial y} + \frac{\partial V}{\partial x} - 2z\frac{\partial^2 W_b}{\partial x \partial y} - 2f(z)\frac{\partial^2 W_s}{\partial x \partial y} \tag{11d}$$

$$\gamma_{xz} = 2\varepsilon_{xz} = g(z)\left(\frac{\partial W_s}{\partial x} + \frac{\partial W_z}{\partial x}\right) \tag{11e}$$

$$\gamma_{yz} = 2\varepsilon_{yz} = g(z)\left(\frac{\partial W_s}{\partial y} + \frac{\partial W_z}{\partial y}\right) \tag{11f}$$

and the curvature tensor is given by substituting Eq. (10) to Eq. (6b):

$$\chi_{xx} = \frac{\partial^2 W_b}{\partial y \partial x} + \frac{1}{2}\left(1 + \frac{\partial f(z)}{\partial z}\right)\frac{\partial^2 W_s}{\partial y \partial x} + \frac{1}{2}g(z)\frac{\partial^2 W_z}{\partial y \partial x} \tag{12a}$$

$$\chi_{yy} = -\frac{\partial^2 W_b}{\partial x \partial y} - \frac{1}{2}\left(1 + \frac{\partial f(z)}{\partial z}\right)\frac{\partial^2 W_s}{\partial x \partial y} - \frac{1}{2}g(z)\frac{\partial^2 W_z}{\partial x \partial y} \tag{12b}$$

$$\chi_{zz} = 0 \tag{12c}$$

$$\chi_{xy} = \frac{1}{2}\left[\frac{\partial^2 W_b}{\partial y^2} - \frac{\partial^2 W_b}{\partial x^2} + \frac{1}{2}\left(1 + \frac{\partial f(z)}{\partial z}\right)\left(\frac{\partial^2 W_s}{\partial y^2} - \frac{\partial^2 W_s}{\partial x^2}\right) + \frac{1}{2}g(z)\left(\frac{\partial^2 W_z}{\partial y^2} - \frac{\partial^2 W_z}{\partial x^2}\right)\right] \tag{12d}$$

$$\chi_{xz} = \frac{1}{4}\left[\frac{\partial^2 \mathrm{V}}{\partial x^2} - \frac{\partial^2 \mathrm{U}}{\partial x \partial y} + \frac{\partial^2 f(z)}{\partial z^2}\frac{\partial W_s}{\partial y} + \frac{\partial g(z)}{\partial z}\frac{\partial W_z}{\partial y}\right] \tag{12e}$$

$$\chi_{yz} = \frac{1}{4}\left[\frac{\partial^2 \mathrm{V}}{\partial x \partial y} - \frac{\partial^2 \mathrm{U}}{\partial y^2} - \frac{\partial^2 f(z)}{\partial z^2}\frac{\partial W_s}{\partial x} - \frac{\partial g(z)}{\partial z}\frac{\partial W_z}{\partial x}\right] \tag{12f}$$

Substituting Eqs. (11) and (12) to Eq. (7), the thermal strain, stress and deviatoric part of couple stress tensors are obtained, respectively:

$$\begin{Bmatrix} \sigma_{xx} \\ \sigma_{yy} \\ \sigma_{zz} \\ \sigma_{xz} \\ \sigma_{yz} \\ \sigma_{xy} \end{Bmatrix} = \begin{bmatrix} Q_{11} & Q_{12} & Q_{12} & 0 & 0 & 0 \\ & Q_{22} & Q_{23} & 0 & 0 & 0 \\ & & Q_{33} & 0 & 0 & 0 \\ & & & Q_{44} & 0 & 0 \\ & & & & Q_{55} & 0 \\ sym. & & & & & Q_{66} \end{bmatrix} \begin{Bmatrix} \frac{\partial U}{\partial x} - z\frac{\partial^2 W_b}{\partial x^2} - f(z)\frac{\partial^2 W_s}{\partial x^2} - \alpha(z,T)\Delta T(x,y,z) \\ \frac{\partial V}{\partial y} - z\frac{\partial^2 W_b}{\partial y^2} - f(z)\frac{\partial^2 W_s}{\partial y^2} - \alpha(z,T)\Delta T(x,y,z) \\ \frac{\partial g(z)}{\partial z}W_z - \alpha(z,T)\Delta T(x,y,z) \\ g(z)\left(\frac{\partial W_s}{\partial x} + \frac{\partial W_z}{\partial x}\right) \\ g(z)\left(\frac{\partial W_s}{\partial y} + \frac{\partial W_z}{\partial y}\right) \\ \frac{\partial U}{\partial y} + \frac{\partial V}{\partial x} - 2z\frac{\partial^2 W_b}{\partial x \partial y} - 2f(z)\frac{\partial^2 W_s}{\partial x \partial y} \end{Bmatrix} \tag{13}$$

$$\begin{Bmatrix} m_{xx} \\ m_{yy} \\ m_{zz} \\ m_{xz} \\ m_{yz} \\ m_{xy} \end{Bmatrix} = 2l^2\mu \begin{Bmatrix} \frac{\partial^2 W_b}{\partial y \partial x} + \frac{1}{2}\left(1+\frac{\partial f(z)}{\partial z}\right)\frac{\partial^2 W_s}{\partial y \partial x} + \frac{1}{2} g(z)\frac{\partial^2 W_z}{\partial y \partial x} \\ -\frac{\partial^2 W_b}{\partial x \partial y} - \frac{1}{2}\left(1+\frac{\partial f(z)}{\partial z}\right)\frac{\partial^2 W_s}{\partial x \partial y} - \frac{1}{2} g(z)\frac{\partial^2 W_z}{\partial x \partial y} \\ 0 \\ \frac{1}{4}\left(\frac{\partial^2 \mathrm{V}}{\partial x^2} - \frac{\partial^2 \mathrm{U}}{\partial x \partial y} + \frac{\partial^2 f(z)}{\partial z^2}\frac{\partial W_s}{\partial y} + \frac{\partial g(z)}{\partial z}\frac{\partial W_z}{\partial y}\right) \\ \frac{1}{4}\left(\frac{\partial^2 \mathrm{V}}{\partial x \partial y} - \frac{\partial^2 \mathrm{U}}{\partial y^2} - \frac{\partial^2 f(z)}{\partial z^2}\frac{\partial W_s}{\partial x} - \frac{\partial g(z)}{\partial z}\frac{\partial W_z}{\partial x}\right) \\ \frac{1}{2}\left[\frac{\partial^2 W_b}{\partial y^2} - \frac{\partial^2 W_b}{\partial x^2} + \frac{1}{2}\left(1+\frac{\partial f(z)}{\partial z}\right)\left(\frac{\partial^2 W_s}{\partial y^2} - \frac{\partial^2 W_s}{\partial x^2}\right) + \frac{1}{2} g(z)\left(\frac{\partial^2 W_z}{\partial y^2} - \frac{\partial^2 W_z}{\partial x^2}\right)\right] \end{Bmatrix} \tag{14}$$

where

$$\left[Q_{ii}, Q_{ij}\right] = \left[Q_{ii}^{2D}, Q_{ij}^{2D}\right] = \begin{cases} \left[\frac{E(z)}{1-\upsilon(z)^2}, \frac{E(z)\upsilon(z)}{1-\upsilon(z)^2}\right]\left(\overline{i,j} = \overline{1,3}\right) \\ \left[\frac{E(z)}{2\left[1+\upsilon(z)\right]}, 0\right]\left(\overline{i,j} = \overline{4,6}\right) \end{cases} \quad \text{for 2D model} \tag{15a}$$

$$\left[Q_{ii}, Q_{ij}\right] = \left[Q_{ii}^{3D}, Q_{ij}^{3D}\right] = \begin{cases} \left[\frac{E(z)\left[1-\upsilon(z)\right]}{\left[1+\upsilon(z)\right]\left[1-2\upsilon(z)\right]}, \frac{E(z)\upsilon(z)}{\left[1+\upsilon(z)\right]\left[1-2\upsilon(z)\right]}\right]\left(\overline{i,j} = \overline{1,3}\right) \\ \left[\frac{E(z)}{2\left[1+\upsilon(z)\right]}, 0\right]\left(\overline{i,j} = \overline{4,6}\right) \end{cases} \quad \text{for quasi-3D model.} \tag{15b}$$

### 2.3. Variational formulation

Hamilton's principle is applied to obtain the equations of motion:

$$\int_{t_1}^{t_2}\left(\delta\Pi + \delta V + \delta K\right)dt \tag{16}$$

where $\delta\Pi, \delta K$ and $\delta V$ denote the variation of strain, kinetic energy and work done by external forces.

The variation of strain energy is rewritten in terms of mid-plane displacements as:

$$\delta\Pi = \int_A \int_{-h/2}^{h/2}\left(\sigma_{ij}\delta\varepsilon_{ij} + m_{ij}\delta\chi_{ij}\right)dzdA$$

$$= \int_A \int_{-h/2}^{h/2} \Big[ \left( \sigma_{xx}\delta\varepsilon_{xx} + \sigma_{yy}\delta\varepsilon_{yy} + \sigma_{zz}\delta\varepsilon_{zz} + \sigma_{xz}\delta\gamma_{xz} + \sigma_{yz}\delta\gamma_{yz} + \sigma_{xy}\delta\gamma_{xy} \right)$$

$$+ \left( m_{xx}\delta\chi_{xx} + m_{yy}\delta\chi_{yy} + m_{zz}\delta\chi_{zz} + 2m_{xz}\delta\chi_{xz} + 2m_{yz}\delta\chi_{yz} + 2m_{xy}\delta\chi_{xy} \right) \Big] dzdA$$

$$= \int_A \Bigg[ \left( N_{xx}\frac{\partial \delta U}{\partial x} - M_{xx}\frac{\partial^2 \delta W_b}{\partial x^2} - P_{xx}\frac{\partial^2 \delta W_s}{\partial x^2} \right) + \left( N_{yy}\frac{\partial \delta V}{\partial y} - M_{yy}\frac{\partial^2 \delta W_b}{\partial y^2} - P_{yy}\frac{\partial^2 \delta W_s}{\partial y^2} \right) + O_{zz}\delta W_z$$

$$+ Q_{xz}\left( \frac{\partial \delta W_s}{\partial x} + \frac{\partial \delta W_z}{\partial x} \right) + Q_{yz}\left( \frac{\partial \delta W_s}{\partial y} + \frac{\partial \delta W_z}{\partial y} \right) + N_{xy}\left( \frac{\partial \delta U}{\partial y} + \frac{\partial \delta V}{\partial x} \right) - 2M_{xy}\frac{\partial^2 \delta W_b}{\partial x \partial y} - 2P_{xy}\frac{\partial^2 \delta W_s}{\partial x \partial y}$$

$$+ R_{xx}\left( \frac{\partial^2 \delta W_b}{\partial x \partial y} + \frac{1}{2}\frac{\partial^2 \delta W_s}{\partial x \partial y} \right) + \frac{1}{2}\left( S_{xx} - S_{yy} \right)\frac{\partial^2 \delta W_s}{\partial x \partial y} + \frac{1}{2}\left( T_{xx} - T_{yy} \right)\frac{\partial^2 \delta W_z}{\partial x \partial y} - R_{yy}\left( \frac{\partial^2 \delta W_b}{\partial x \partial y} + \frac{1}{2}\frac{\partial^2 \delta W_s}{\partial x \partial y} \right)$$

$$+ \frac{1}{2}R_{xz}\left( \frac{\partial^2 V}{\partial x^2} - \frac{\partial^2 U}{\partial x \partial y} \right) + \frac{1}{2}R_{yz}\left( \frac{\partial^2 V}{\partial x \partial y} - \frac{\partial^2 U}{\partial y^2} \right) + \frac{1}{2}X_{xz}\left( \frac{\partial W_s}{\partial y} + \frac{\partial W_z}{\partial y} \right) - \frac{1}{2}X_{yz}\left( \frac{\partial W_s}{\partial x} + \frac{\partial W_z}{\partial x} \right)$$

$$+ \frac{1}{2}R_{xy}\left( \frac{\partial^2 W_b}{\partial y^2} - \frac{\partial^2 W_b}{\partial x^2} \right) + \frac{1}{2}R_{xy}\left( \frac{\partial^2 W_s}{\partial y^2} - \frac{\partial^2 W_s}{\partial x^2} \right) + \frac{1}{2}S_{xy}\left( \frac{\partial^2 W_s}{\partial y^2} - \frac{\partial^2 W_s}{\partial x^2} \right) + \frac{1}{2}T_{xy}\left( \frac{\partial^2 W_z}{\partial y^2} - \frac{\partial^2 W_z}{\partial x^2} \right) \Bigg] dA \tag{17}$$

where the stress resultants are expressed as:

$$\left( N_{ij}, M_{ij}, P_{ij}, Q_{ij}, O_{ij} \right) = \int_{-h/2}^{h/2} \left( 1, z, f(z), g(z), \frac{\partial g(z)}{\partial z} \right) \sigma_{ij} dz - \left( N_{ij}^T, M_{ij}^T, P_{ij}^T, 0, O_{ij}^T \right) \tag{18a}$$

$$\left( R_{ij}, S_{ij}, T_{ij}, X_{ij} \right) = \int_{-h/2}^{h/2} \left( 1, \frac{\partial f(z)}{\partial z}, g(z), \frac{\partial^2 f(z)}{\partial z^2} \right) m_{ij} dz \tag{18b}$$

where

$$\left( N_{ij}^T, M_{ij}^T, P_{ij}^T, O_{ij}^T \right) = \int_{-h/2}^{h/2} \left( 1, z, f(z), \frac{\partial g(z)}{\partial z} \right) \left( Q_{ii} + 2Q_{ij} \right) \alpha(z,T) \Delta T(z) dz, \left( \overline{i,j} = \overline{1,3} \right) \tag{19}$$

It is noticeable that the integration is written for FG plate only, for sandwich plate cumulative formulation is applied, i.e. $\int_{-h/2}^{h/2} \mathbb{F}(z)dz = \int_{h_0}^{h_1} \mathbb{F}(z)dz + \int_{h_1}^{h_2} \mathbb{F}(z)dz + \int_{h_2}^{h_3} \mathbb{F}(z)dz$ where $\mathbb{F}(z)$ is an arbitrary function of $z$.

Substituting Eqs. (13), (14) and (19) into Eq. (18), the stress resultants can be described in terms of mid-plane displacements as in the Appendix.

The variation of the work done by transverse load $q$ and in-plane load $P_0$ is presented as:

$$\delta V = -\int_A \left[ P_0 \left[ \delta W_b' \left( W_b' + W_s' \right) + \delta W_s' \left( W_b' + W_s' \right) \right] + q\left( \delta W_b + \delta W_s + g\delta W_z \right) \right] dA \tag{20}$$

The variation of kinetic energy is presented by:

$$\delta K=\int_A\int_{-h/2}^{h/2}\rho\left(z\right)\left(\dot{u}_1\delta\dot{u}_1+\dot{u}_2\delta\dot{u}_2+\dot{u}_3\delta\dot{u}_3\right)dzdA$$

$$=\int_A\left\{I_0\left[\dot{U}\delta\dot{U}+\dot{V}\delta\dot{V}+\left(\dot{W}_b+\dot{W}_s\right)\delta\left(\dot{W}_b+\dot{W}_s\right)\right]+J_0\left[\left(\dot{W}_b+\dot{W}_s\right)\delta\dot{W}_z+\dot{W}_z\delta\left(\dot{W}_b+\dot{W}_s\right)\right]\right.$$

$$-I_1\left(\dot{U}\frac{\partial\delta\dot{W}_b}{\partial x}+\frac{\partial\dot{W}_s}{\partial x}\delta\dot{U}+\dot{V}\frac{\partial\delta\dot{W}_b}{\partial y}+\frac{\partial\dot{W}_b}{\partial y}\delta\dot{V}\right)+I_2\left(\frac{\partial\dot{W}_b}{\partial x}\frac{\partial\delta\dot{W}_b}{\partial x}+\frac{\partial\dot{W}_b}{\partial y}\frac{\partial\delta\dot{W}_b}{\partial y}\right)$$

$$-J_1\left(\dot{U}\frac{\partial\delta\dot{W}_s}{\partial x}+\frac{\partial\dot{W}_s}{\partial x}\delta\dot{U}+\dot{V}\frac{\partial\delta\dot{W}_s}{\partial y}+\frac{\partial\dot{W}_s}{\partial y}\delta\dot{V}\right)+K_2\left(\frac{\partial\dot{W}_s}{\partial x}\frac{\partial\delta\dot{W}_s}{\partial x}+\frac{\partial\dot{W}_s}{\partial y}\frac{\partial\delta\dot{W}_s}{\partial y}\right)$$

$$\left.+J_2\left(\frac{\partial\dot{W}_b}{\partial x}\frac{\partial\delta\dot{W}_s}{\partial x}+\frac{\partial\dot{W}_s}{\partial x}\frac{\partial\delta\dot{W}_b}{\partial x}+\frac{\partial\dot{W}_b}{\partial y}\frac{\partial\delta\dot{W}_s}{\partial y}+\frac{\partial\dot{W}_s}{\partial y}\frac{\partial\delta\dot{W}_b}{\partial y}\right)+K_0\dot{W}_z\delta\dot{W}_z\right\}dA \tag{21}$$

where

$$\left(I_0,I_1,I_2,J_0,J_1,J_2,K_0,K_2\right)=\int_{-h/2}^{h/2}\left(1,z,z^2,g\left(z\right),f\left(z\right),zf\left(z\right),g^2\left(z\right),f^2\left(z\right)\right)\rho\left(z\right)dz \tag{22}$$

Substituting Eqs. (17), (20) and (21) into Eq. (16), integrating by parts and gathering the coefficients of $\delta U,\delta V,\delta W_b,\delta W_s$ and $\delta W_z$, the equations of motion can be obtained:

$$\frac{\partial N_{xx}}{\partial x}+\frac{\partial N_{xy}}{\partial y}+\frac{1}{2}\frac{\partial^2 R_{xz}}{\partial x\partial y}+\frac{1}{2}\frac{\partial^2 R_{yz}}{\partial y^2}=I_0\ddot{U}-I_1\frac{\partial\ddot{W}_b}{\partial x}-J_1\frac{\partial\ddot{W}_s}{\partial x} \tag{23a}$$

$$\frac{\partial N_{yy}}{\partial y}+\frac{\partial N_{xy}}{\partial x}-\frac{1}{2}\frac{\partial^2 R_{xz}}{\partial x^2}-\frac{1}{2}\frac{\partial^2 R_{yz}}{\partial x\partial y}=I_0\ddot{V}-I_1\frac{\partial\ddot{W}_b}{\partial y}-J_1\frac{\partial\ddot{W}_s}{\partial y} \tag{23b}$$

$$\frac{\partial^2 M_{xx}}{\partial x^2}+\frac{\partial^2 M_{yy}}{\partial y^2}+2\frac{\partial^2 M_{xy}}{\partial x\partial y}-\frac{\partial^2 R_{xx}}{\partial x\partial y}+\frac{\partial^2 R_{yy}}{\partial x\partial y}-\frac{\partial^2 R_{xy}}{\partial y^2}+\frac{\partial^2 R_{xy}}{\partial x^2}+P_0+q$$

$$=I_0\left(\ddot{W}_b+\ddot{W}_s\right)+J_0\ddot{\varphi}_z+I_1\left(\frac{\partial\ddot{U}}{\partial x}+\frac{\partial\ddot{V}}{\partial y}\right)-I_2\nabla^2\ddot{W}_b-J_2\nabla^2\ddot{W}_s \tag{23c}$$

$$\frac{\partial^2 P_{xx}}{\partial x^2}+\frac{\partial^2 P_{yy}}{\partial y^2}+\frac{\partial Q_{yz}}{\partial y}+\frac{\partial Q_{xz}}{\partial x}+2\frac{\partial^2 P_{xy}}{\partial x\partial y}-\frac{1}{2}\frac{\partial^2 R_{xx}}{\partial x\partial y}-\frac{1}{2}\frac{\partial^2 S_{xx}}{\partial x\partial y}+\frac{1}{2}\frac{\partial^2 R_{yy}}{\partial x\partial y}+\frac{1}{2}\frac{\partial^2 S_{yy}}{\partial x\partial y}$$

$$+\frac{1}{2}\frac{\partial X_{xz}}{\partial y}-\frac{1}{2}\frac{\partial X_{yz}}{\partial x}-\frac{1}{2}\frac{\partial^2 R_{xy}}{\partial y^2}-\frac{1}{2}\frac{\partial^2 S_{xy}}{\partial y^2}+\frac{1}{2}\frac{\partial^2 R_{xy}}{\partial x^2}+\frac{1}{2}\frac{\partial^2 S_{xy}}{\partial x^2}+P_0+q$$

$$=I_0\left(\ddot{W}_b+\ddot{W}_s\right)+J_0\ddot{\varphi}_z+J_1\left(\frac{\partial\ddot{U}}{\partial x}+\frac{\partial\ddot{V}}{\partial y}\right)-J_2\nabla^2\ddot{W}_b-K_2\nabla^2\ddot{W}_s \tag{23d}$$

$$-O_{zz}+\frac{\partial Q_{xz}}{\partial x}+\frac{\partial Q_{yz}}{\partial y}-\frac{1}{2}\frac{\partial^2 T_{xx}}{\partial x\partial y}+\frac{1}{2}\frac{\partial^2 T_{yy}}{\partial x\partial y}-\frac{1}{2}\frac{\partial X_{xz}}{\partial y}+\frac{1}{2}\frac{\partial X_{yz}}{\partial x}-\frac{1}{2}\frac{\partial^2 T_{xy}}{\partial y^2}+\frac{1}{2}\frac{\partial^2 T_{xy}}{\partial x^2}+gq$$

$$=J_0\left(\ddot{W}_b+\ddot{W}_s\right)+K_0\ddot{\varphi}_z \tag{23e}$$

where $\nabla^2 = \frac{\partial^2}{\partial x^2} + \frac{\partial^2}{\partial y^2}$ , $P_0 = P_x^0 \frac{\partial^2 \left(W_b + W_s\right)}{\partial x^2} + P_y^0 \frac{\partial^2 \left(W_b + W_s\right)}{\partial y^2} + P_{xy}^0 \frac{\partial^2 \left(W_b + W_s\right)}{\partial x \partial y}$

in which $P_x^0, P_y^0$ and $P_{xy}^0$ are the in-plane mechanical/thermal equivalent forces (in vibration and buckling analysis).

The governing equations are expressed in terms of displacements as:

$$A_{11} \frac{\partial^2 U}{\partial x^2} + A_{66} \frac{\partial^2 U}{\partial y^2} - \frac{1}{4} A_m \left( \frac{\partial^4 U}{\partial x^2 \partial y^2} + \frac{\partial^4 U}{\partial y^4} \right) + \left(A_{12} + A_{66}\right) \frac{\partial^2 V}{\partial x \partial y} + \frac{1}{4} A_m \left( \frac{\partial^4 V}{\partial x^3 \partial y} + \frac{\partial^4 V}{\partial x \partial y^3} \right) - B_{11} \frac{\partial^3 W_b}{\partial x^3}$$
$$-\left(B_{12} + 2B_{66}\right) \frac{\partial^3 W_b}{\partial x \partial y^2} - B_{11}^s \frac{\partial^3 W_s}{\partial x^3} - \left(B_{12}^s + 2B_{66}^s\right) \frac{\partial^3 W_s}{\partial x \partial y^2} + K_{13} \frac{\partial \varphi_z}{\partial x} - \frac{\partial N_{xx}^T}{\partial x} = I_0 \ddot{U} - I_1 \frac{\partial \ddot{W}_b}{\partial x} - J_1 \frac{\partial \ddot{W}_s}{\partial x} \tag{24a}$$

$$A_{22} \frac{\partial^2 V}{\partial y^2} + A_{66} \frac{\partial^2 V}{\partial x^2} - \frac{1}{4} A_m \left( \frac{\partial^4 V}{\partial x^4} + \frac{\partial^4 V}{\partial x^2 \partial y^2} \right) + \left(A_{12} + A_{66}\right) \frac{\partial^2 U}{\partial x \partial y} + \frac{1}{4} A_m \left( \frac{\partial^4 U}{\partial x^3 \partial y} + \frac{\partial^4 U}{\partial x \partial y^3} \right) - B_{22} \frac{\partial^3 W_b}{\partial y^3}$$
$$-\left(B_{12} + 2B_{66}\right) \frac{\partial^3 W_b}{\partial x^2 \partial y} - B_{22}^s \frac{\partial^3 W_s}{\partial y^3} - \left(B_{12}^s + 2B_{66}^s\right) \frac{\partial^3 W_s}{\partial x^2 \partial y} + K_{23} \frac{\partial \varphi_z}{\partial y} - \frac{\partial N_{yy}^T}{\partial y} = I_0 \ddot{V} - I_1 \frac{\partial \ddot{W}_b}{\partial y} - J_1 \frac{\partial \ddot{W}_s}{\partial y} \tag{24b}$$

$$B_{11} \frac{\partial^3 U}{\partial x^3} + \left(B_{12} + 2B_{66}\right) \frac{\partial^3 U}{\partial x \partial y^2} + \left(B_{12} + 2B_{66}\right) \frac{\partial^3 V}{\partial x^2 \partial y} + B_{22} \frac{\partial^3 V}{\partial y^3} - \left(D_{11} + A_m\right) \frac{\partial^4 W_b}{\partial x^4}$$
$$-\left(2D_{12} + 4D_{66} + 2A_m\right) \frac{\partial^4 W_b}{\partial x^2 \partial y^2} - \left(D_{22} + A_m\right) \frac{\partial^4 W_b}{\partial y^4} - \left[ D_{11}^s + \frac{1}{2}\left(A_m + B_m\right) \right] \frac{\partial^4 W_s}{\partial x^4}$$
$$-\left(2D_{12}^s + 4D_{66}^s\right) \frac{\partial^4 W_s}{\partial x^2 \partial y^2} - \left[ D_{22}^s + \frac{1}{2}\left(A_m + B_m\right) \right] \frac{\partial^4 W_s}{\partial y^4} + L_{13} \frac{\partial^2 \varphi_z}{\partial x^2}$$
$$+L_{23} \frac{\partial^2 \varphi_z}{\partial y^2} - \frac{1}{2} E_m \frac{\partial^4 \varphi_z}{\partial x^4} - \frac{1}{2} E_m \frac{\partial^4 \varphi_z}{\partial y^4} + P_0 + q - \frac{\partial^2 M_{xx}^T}{\partial x^2} - \frac{\partial^2 M_{yy}^T}{\partial y^2}$$
$$= I_0 \left(\ddot{W}_b + \ddot{W}_s\right) + I_1 \left( \frac{\partial \ddot{U}}{\partial x} + \frac{\partial \ddot{V}}{\partial y} \right) - I_2 \nabla^2 \ddot{W}_b - J_2 \nabla^2 \ddot{W}_s + J_0 \ddot{\varphi}_z \tag{24c}$$

$$B_{11}^s \frac{\partial^3 U}{\partial x^3} + \left(B_{12}^s + 2B_{66}^s\right) \frac{\partial^3 U}{\partial x \partial y^2} + \left(B_{12}^s + 2B_{66}^s\right) \frac{\partial^3 V}{\partial x^2 \partial y} + B_{22}^s \frac{\partial^3 V}{\partial y^3}$$
$$-\left[ D_{11}^s + \frac{1}{2}\left(A_m + B_m\right) \right] \frac{\partial^4 W_b}{\partial x^4} - \left(2D_{12}^s + 4D_{66}^s\right) \frac{\partial^4 W_b}{\partial x^2 \partial y^2} - \left[ D_{22}^s + \frac{1}{2}\left(A_m + B_m\right) \right] \frac{\partial^4 W_b}{\partial y^4}$$
$$+\left( A_{55}^s + \frac{1}{4} H_m \right) \frac{\partial^2 W_s}{\partial x^2} + \left( A_{44}^s + \frac{1}{4} H_m \right) \frac{\partial^2 W_s}{\partial y^2} - \left[ H_{11} + \frac{1}{4}\left(A_m + 2B_m + C_m\right) \right] \frac{\partial^4 W_s}{\partial x^4}$$
$$-\left(2H_{12} + 4H_{66}\right) \frac{\partial^4 W_s}{\partial x^2 \partial y^2} - \left[ H_{22} + \frac{1}{4}\left(A_m + 2B_m + C_m\right) \right] \frac{\partial^4 W_s}{\partial y^4}$$
$$+\left( L_{13}^s + A_{55}^s - \frac{1}{4} H_m \right) \frac{\partial^2 \varphi_z}{\partial x^2} + \left( L_{23}^s + A_{44}^s - \frac{1}{4} H_m \right) \frac{\partial^2 \varphi_z}{\partial y^2} - \frac{1}{4}\left(D_m + E_m\right) \left( \frac{\partial^4 \varphi_z}{\partial x^4} + \frac{\partial^4 \varphi_z}{\partial y^4} \right)$$
$$+P_0 + q - \frac{\partial^2 P_{xx}^T}{\partial x^2} - \frac{\partial^2 P_{yy}^T}{\partial y^2} = I_0 \left(\ddot{W}_b + \ddot{W}_s\right) + J_1 \left( \frac{\partial \ddot{U}}{\partial x} + \frac{\partial \ddot{V}}{\partial y} \right) - J_2 \nabla^2 \ddot{W}_b - K_2 \nabla^2 \ddot{W}_s + J_0 \ddot{\varphi}_z \tag{24d}$$

$$-K_{13}\frac{\partial U}{\partial x}-K_{23}\frac{\partial V}{\partial y}+L_{13}\frac{\partial^2 W_b}{\partial x^2}+L_{23}\frac{\partial^2 W_b}{\partial y^2}-\frac{1}{2}E_m\frac{\partial^4 W_b}{\partial x^4}-\frac{1}{2}E_m\frac{\partial^4 W_b}{\partial y^4}$$
$$+\left(L_{13}^s+A_{55}^s-\frac{1}{4}H_m\right)\frac{\partial^2 W_s}{\partial x^2}+\left(L_{23}^s+A_{44}^s-\frac{1}{4}H_m\right)\frac{\partial^2 W_s}{\partial y^2}-\frac{1}{4}\left(E_m+D_m\right)\frac{\partial^4 W_s}{\partial x^4}$$
$$-\frac{1}{4}\left(E_m+D_m\right)\frac{\partial^4 W_s}{\partial y^4}-Z_{33}\varphi_z+\left(A_{55}^s+\frac{1}{4}H_m\right)\frac{\partial^2\varphi_z}{\partial x^2}$$
$$+\left(A_{44}^s+\frac{1}{4}H_m\right)\frac{\partial^2\varphi_z}{\partial y^2}-\frac{1}{4}F_m\left(\frac{\partial^4\varphi_z}{\partial x^4}+\frac{\partial^4\varphi_z}{\partial y^4}\right)+gq+O_{zz}^T=J_0\left(\ddot{W}_b+\ddot{W}_s\right)+K_0\ddot{\varphi}_z \tag{24e}$$

## 3. Analytical solution

Based on the Navier approach, the displacements are expressed in terms of Fourier series as:

$$U(x,y)=\sum_{n=1}^{\infty}\sum_{m=1}^{\infty}U_{mn}\cos\alpha x\sin\beta y \tag{25a}$$

$$V(x,y)=\sum_{n=1}^{\infty}\sum_{m=1}^{\infty}V_{mn}\sin\alpha x\cos\beta y \tag{25b}$$

$$W_b(x,y)=\sum_{n=1}^{\infty}\sum_{m=1}^{\infty}W_{bmn}\sin\alpha x\sin\beta y \tag{25c}$$

$$W_s(x,y)=\sum_{n=1}^{\infty}\sum_{m=1}^{\infty}W_{smn}\sin\alpha x\sin\beta y \tag{25d}$$

$$W_z(x,y)=\sum_{n=1}^{\infty}\sum_{m=1}^{\infty}W_{zmn}\sin\alpha x\sin\beta y \tag{25e}$$

where $\alpha=m\pi/a,\beta=n\pi/b$ and $\left(U_{nm},V_{nm},W_{bnm},W_{snm},W_{znm}\right)$ are coefficients. Similarly, mechanical/ thermal loads are expanded as:

$$q(x,y)=\sum_{n=1}^{\infty}\sum_{m=1}^{\infty}q_{mn}\sin\alpha x\sin\beta y \tag{26a}$$

$$\Delta T_i(x,y)=\sum_{n=1}^{\infty}\sum_{m=1}^{\infty}\Delta T_{imn}\sin\alpha x\sin\beta y,(i=1,2) \tag{26b}$$

and

$$\left(q_{mn},\Delta T_{imn}\right)=\left(q_0,\Delta T_i\right)\text{ for sinusoidally distributed loads} \tag{27a}$$

$$\left(q_{mn},\Delta T_{imn}\right)=\frac{16}{nm\pi^2}\left(q_0,\Delta T_i\right)\text{ for uniformly distributed loads} \tag{27b}$$

Substituting Eqs. (23) and (24) to Eq. (18), governing equations can be rewritten as:

$$\left(k_{ij}-m_{ij}\omega^2\right)\left\{u_{jmn}\right\}=\left\{F_{jmn}\right\},\text{where } k_{ij}=k_{ji};m_{ij}=m_{ji}\left(\overline{i,j=1,5}\right) \tag{28}$$

where

$$k_{11}=-A_{11}\alpha^2-A_{66}\beta^2-\frac{1}{4}A_m\left(\alpha^2\beta^2+\beta^4\right);\; k_{12}=-\left(A_{12}+A_{66}\right)\alpha\beta+\frac{1}{4}A_m\left(\alpha^3\beta+\alpha\beta^3\right);$$

$$k_{13}=B_{11}\alpha^3+\left(B_{12}+2B_{66}\right)\alpha\beta^2;\; k_{14}=B_{11}^s\alpha^3+\left(B_{12}^s+2B_{66}^s\right)\alpha\beta^2;\; k_{15}=K_{13}\alpha$$

$$k_{22}=-A_{22}\beta^2-A_{66}\alpha^2-\frac{1}{4}A_m\left(\alpha^4+\alpha^2\beta^2\right);\; k_{23}=B_{22}\beta^3+\left(B_{12}+2B_{66}\right)\alpha^2\beta;$$

$$k_{24}=B_{22}^s\beta^3+\left(B_{12}^s+2B_{66}^s\right)\alpha^2\beta;\; k_{25}=K_{23}\beta$$

$$k_{33}=-\left(D_{11}+A_m\right)\alpha^4-\left(2D_{12}+4D_{66}+2A_m\right)\alpha^2\beta^2-\left(D_{22}+A_m\right)\beta^4-\left(\alpha^2+\beta^2\right)P_0$$

$$k_{34}=-\left[D_{11}^s+\frac{1}{2}\left(A_m+B_m\right)\right]\alpha^4-\left[2D_{12}^s+4D_{66}^s+\left(A_m+B_m\right)\right]\alpha^2\beta^2-\left[D_{22}^s+\frac{1}{2}\left(A_m+B_m\right)\right]\beta^4$$
$$-\left(\alpha^2+\beta^2\right)P_0$$

$$k_{35}=-L_{13}\alpha^2-L_{23}\beta^2-\frac{1}{2}E_m\left(\alpha^2+\beta^2\right)^2$$

$$k_{44}=-\left(A_{55}^s-\frac{1}{4}H_m\right)\alpha^2-\left(A_{44}^s+\frac{1}{4}H_m\right)\beta^2-\left(H_{11}+\frac{1}{4}\left(A_m+2B_m+C_m\right)\right)\alpha^4-\left(2H_{12}+4H_{66}\right)\alpha^2\beta^2$$
$$-\left(H_{22}+\frac{1}{4}\left(A_m+2B_m+C_m\right)\right)\beta^4-\left(\alpha^2+\beta^2\right)P_0$$

$$k_{45}=-\left(L_{13}^s+A_{55}^s-\frac{1}{4}H_m\right)\alpha^2-\left(L_{23}^s+A_{44}^s-\frac{1}{4}H_m\right)\beta^2-\frac{1}{4}\left(D_m+E_m\right)\left(\alpha^2+\beta^2\right)^2$$

$$k_{55}=-Z_{33}-\left(A_{55}^s+\frac{1}{4}H_m\right)\alpha^2-\left(A_{44}^s+\frac{1}{4}H_m\right)\beta^2-\frac{1}{4}F_m\left(\alpha^2+\beta^2\right)^2 \tag{29a}$$

$$m_{11}=I_0;\; m_{13}=-I_1\alpha;\; m_{14}=-J_1\alpha;\; m_{22}=I_0;\; m_{23}=-I_1\beta;\; m_{24}=-J_1\beta$$

$$m_{33}=I_0+I_2\left(\alpha^2+\beta^2\right);\; m_{34}=I_0+J_2\left(\alpha^2+\beta^2\right);\; m_{35}=J_0$$

$$m_{44}=I_0+K_2\left(\alpha^2+\beta^2\right);\; m_{45}=J_0;\; m_{45}=K_0;\; m_{12}=m_{15}=m_{25}=0 \tag{29b}$$

$$F_j=\left\{F_1,F_2,F_3,F_4,F_5\right\}$$

$$F_1=-\alpha\left(A_t\Delta T_1+B_t\frac{\Delta T_2}{h}\right);\; F_2=-\beta\left(A_t\Delta T_1+B_t\frac{\Delta T_2}{h}\right);\; F_3=\left(\alpha^2+\beta^2\right)\left(B_t\Delta T_1+D_t\frac{\Delta T_2}{h}\right)$$

$$F_4=\left(\alpha^2+\beta^2\right)\left(B_t^s\Delta T_1+D_t^s\frac{\Delta T_2}{h}\right);\; F_5=\left(C_t\Delta T_1+C_t^s\frac{\Delta T_2}{h}\right) \tag{29c}$$

In bending behaviour, the mid-plane displacements are simply calculated by $\left\{u_{jmn}\right\}=k_{ij}\setminus\left\{F_{jmn}\right\}$, where $\left(m,n\right)=\left(1,1\right)$ for the in-plane sinusoidal temperature and $\left(m,n\right)=\left(\overline{1-19},\overline{1-19}\right)$ for the in-plane uniform temperature. It should be noted that the increase of temperature results in the change of material properties and the thermal stress resultants, which leads to the forced vibration and nonlinear buckling analysis. In this paper, only in-plane thermal resultant (axial force) is considered which enable to solve the problems using eigenvalue algorithm. The thermal vibration and buckling behaviours are similar to mechanical behaviours including the temperature-dependent material properties, thus a trial and error procedure needs to be applied to obtain the critical buckling temperatures.

**4. Numerical results and discussion**

In this session, numerical examples are carried out to study the bending, vibration and buckling behaviours of FG sandwich microplates under mechanical and thermal loads. Firstly, verification is presented for microplates under mechanical loads and macroplates under thermal loads. Differences between constitutive relations as well as between Third-order Shear Deformation Theory (TSDT) and Sinusoidal Shear Deformation Theory (SSDT) is also discussed. Parameter study is then conducted to investigate the thermal behaviours of FG sandwich microplates. In these examples, effects of geometric configurations and temperatures on microplates are investigated using both 2D and quasi-3D models. Apart from the temperature-independent (TID) form, which is applied to verify the present solution, the temperature-dependent (TD) form is considered in the rest of this work. Material properties for mechanical and TD coefficients for thermal analysis are presented in Tables 1 and 2. Non-dimensional expressions used in this paper are:

Bending:

Mechanical load:

Deflection: $$\bar{w}(z)=\frac{10E_c h^3}{q_0 a^4}u_3\left(\frac{a}{2},\frac{b}{2},z\right) \tag{30a}$$

Stress: $$\bar{\sigma}_{xx}=\frac{h\sigma_{xx}}{aq_0},\ \bar{\sigma}_{xz}=\frac{h\sigma_{xz}}{aq_0} \tag{30b}$$

Thermal load:

Deflection: $$\bar{w}(z)=\frac{h}{\alpha_0\Delta T_2 a^2}u_3\left(\frac{a}{2},\frac{b}{2},z\right) \tag{30c}$$

Stress: $$\bar{\sigma}_{xx}=\frac{h^2}{\alpha_0\Delta T_2 E_0 a^2}\sigma_{xx}\left(\frac{a}{2},\frac{b}{2},z\right) \tag{30d}$$

where $E_0=1GPa,\alpha_0=10^{-6}\ {}^0C^{-1}$

Vibration: $$\hat{\omega}=\frac{\omega a^2}{h}\sqrt{\frac{\rho_c}{E_c}},\ \bar{\omega}=\frac{\omega a^2}{h}\sqrt{\frac{\rho_0\left(1-\upsilon_0^2\right)}{E_0}} \tag{30e}$$

Buckling: $$\bar{P}_{cr} = P_{cr}\frac{a^2}{E_0 h^3} \tag{30f}$$

where $E_0, \rho_0$ and $\upsilon_0$ are the Young's modulus, mass density and Poisson's ratio of metal at 300K.

*4.1. Verification:*

*a. Static bending analysis:*

Table 3 validates the obtained solutions of transverse displacement $\bar{w}$ and normal stress $\bar{\sigma}_{xx}$ under mechanical load for microplates. The sinusoidal mechanical load is applied to $Al/Al_2O_3$ plate with different slenderness ratios and power-law indices. Under mechanical load, the present quasi-3D results are in good agreement with other quasi-3D ones. Considering 2D models, Lei et al. [38] degenerated quasi-3D to 2D model by setting $W_z$ to zero, which results in a slight difference in stress $\bar{\sigma}_{xx}$ compared to present solutions and those obtained by Thai and Vo [25]. It is also seen that quasi-3D models provide higher deflections for small-scale plates but lower values for thicker plates compared to 2D models. Further verification is presented for thermal bending of FG sandwich macroplates. By applying the linear temperature through the thickness, the deflections and stresses of Ti-6Al-4V/$ZrO_2$ plates are presented in Table 4. It is seen that the present TSDT and SSDT results are in excellent agreement with those obtained from Tounsi et al. [39] while the quasi-3D ones agree well with those reported by Mantari and Granados [40]. It should be noted that the 2D constitutive relation, i.e. $\left[Q_{ii}^{2D}, Q_{ij}^{2D}\right]$, was applied to the quasi-3D solution in [40]. In this example, applying quasi-3D theories not only increases the stiffness but also induces the load component $F_5$ which is caused by z-direction thermal stretching. Therefore, thermal deflections achieved from quasi-3D models together with $\left[Q_{ii}^{3D}, Q_{ij}^{3D}\right]$ are higher than those from 2D models. At the same time, between SSDT and TSDT which are employed to quasi-3D models, the former provides higher stress magnitudes and the difference is much more pronounced in thermal case. Those values from SSDT quasi-3D model are comparable to the results obtained from 2D solutions. In this paper, SSDT is applied to static bending behaviours while TSDT is applied to vibration and buckling analysis.

*b. Vibration and buckling analysis:*

Fundamental frequencies of $Al/Al_2O_3$ microplates are compared with those of Lei et al. [38] in Table 5 and presented in Fig. 2 for various slenderness and material length scale ratios. Excellent agreement can be observed. In addition, the natural frequencies reduce with higher material length scale ratios and level out as $h/l \geq 20$. With respect to the thermal effect, the vibration of $Si_3N_4$/SUS304 macroplates $(a/h = 10)$ under uniform temperature is verified with those given in [41] considering TID and TD forms in Table 6. In this example, the equivalent axial load caused by the thermal stress is calculated with/without the transverse thermal stress $\sigma_{zz}^{T}$ (either $\left[Q_{ii}^{3D}, Q_{ij}^{3D}\right]$ or $\left[Q_{ii}^{2D}, Q_{ij}^{2D}\right]$ is utilised for thermal stress, respectively). The present TSDT results are almost the same with those in [41] while the quasi-3D solution provides lower natural frequencies, especially when $\sigma_{zz}^{T}$ is included. The TD solution, which describes better the working status of materials, also displays lower natural frequencies compared to TID one.

Further verification is carried out for mechanical and thermal buckling behaviours of FG plates in Tables 7 and 8. As can be seen in Table 7, the present results of mechanical buckling agree well with those obtained from refined plate theories (RPT) [26, 28] and quasi-3D theory [28]. It is also shown that the inclusion of normal stretching effect leads to the higher critical buckling loads for macroplates but less significant to microplates. Regarding the thermal buckling behaviour, by applying the linear temperature which is expressed by $T(x,y,z)=305+(1/2+z/h)\Delta T$ [31], a good agreement can be seen for $Al/Al_2O_3$ macroplates and thin microplates in Table 8. This temperature pattern, which assumes the temperature elevation occurs only at the top surface, can lead to a very high difference in the temperature at the bottom and top surfaces; therefore, the temperature distribution described in Eq. (4) and the exclusion of $\sigma_{zz}^{T}$ are considered in the thermal vibration and buckling analysis.

*4.2. Parameter study:*

*a. Static bending analysis:*

The deflection and stress of Ti-6Al-4V/$ZrO_2$ plates under various thickness scales and temperatures is presented in Fig. 3. In this figure, TID is considered to verify with those obtained from [40] for the macroplates under the higher temperatures. The small-scale effect can be seen for deflection and stress in microplates and is negligible for thicker plates $(h \geq 20l)$ where a good agreement with those results for macroplates is observed. Regarding the thickness stretching effect, the results from the quasi-3D and 2D models agree well at ambient temperature but the significant difference between them is observed at elevated temperature. In addition, under lower temperature, the positive deflection can be seen while the negative deflection is obtained with increasing temperature. This can be explained by the difference in thermal expansions of Ti-6Al-4V and $ZrO_2$. At the lower temperature, the linear temperature causes an expansion on the upper face (ceramic – $ZrO_2$) whereas the metal has not been heated up. This results in a coupled force pushing the plate upward. At the higher temperature $\Delta T_1$, due to the higher thermal expansion coefficient, the metal surface stretches more than the ceramic one which creates a reverse moment pushing the plate downward. This change is illustrated by the transverse displacements obtained from quasi-3D and 2D models for various thickness scales in Fig. 4. It is seen that the difference between these solutions are more profound under thermal loads than under mechanical loads.

Tables 9 and 10 present the non-dimensional deflection of $Si_3N_4$/SUS304 sandwich microplates under uniform and linear temperatures through the thickness. No displacement is shown in Table 9 for homogeneous plates (FG or homogeneous-core sandwich plate with $p=0$) due to the symmetry of material and thermal stress under uniform temperature. The deflection increases with respect to temperature but in different ways, upward for the ceramic-core plates and downward for the others. Also, less deflection can be observed for smaller scale plates under thermal environment, which is similar to the case of mechanical loads. At the macro scale, smallest displacement is observed in metal-core plates, especially under uniform temperature. At the micro scale, the homogeneous-core plates induce lower deflection under uniform temperature, but higher deflection under linear temperature compared to the FG/ FG-core plates. To compare the quasi-3D and 2D models in evaluating thermal stresses, Fig. 5 displays the through-the-thickness normal and shear stresses of sandwich microplates under thermal environment. The inclusion of stretching effect leads to the higher stresses and this difference is more significant at the top and bottom surfaces for the normal stress and at the middle surface for the shear stress. The stress distributions under uniform and linear temperatures are revealed in Fig. 6. The linear temperature results in the higher normal stress at the top surface but the lower at the bottom surface compared to the uniform temperature. In addition, the higher shear stresses are obtained under uniform temperature for FG-core plates but under linear temperature for the homogeneous-core plates. In increasing the material length scales ratio, the shear stresses reduce significantly and the normal stress also changes the distribution, from higher at the top to higher at the bottom.

*b. Vibration and buckling analysis:*

The natural frequencies under uniform and linear temperatures are presented for $Si_3N_4$/SUS304 microplates $\left(a/h=10, p=1\right)$ in Fig. 7 with TD solution. In this example, $\left[Q_{ii}^{3D}, Q_{ij}^{3D}\right]$ relation is applied for thermal stress in evaluating equivalent axial loads. As expected, the natural frequency decreases as increasing temperature up to zero at the critical buckling temperature. In addition, the difference between the natural frequencies under uniform and linear temperatures is minor, but the difference between 2D and quasi-3D solutions increases with elevated temperature. Considering the small-scale effect, the smaller material length scale ratios are considered, the higher natural frequencies are obtained. This can be explained that including the deviatoric part of the symmetric couple stress tensors in strain energy strengthen the stiffness of the microplates. The natural frequencies of sandwich microplates under thermal environment are presented in Fig. 8 and Tables 11-13 for FG-, ceramic- and metal- core, respectively. Under both uniform and linear temperatures, the highest natural frequencies can be seen in ceramic-core and the lowest in metal-core plates. In addition, the increase of power-law index leads to the lower natural frequencies in FG-core and ceramic-core plates but the higher natural frequencies in metal-core plates. Finally, the critical buckling temperatures are tabulated in Table 14 for $Si_3N_4$/SUS304 microplates. As expected, the higher values are observed for smaller material length scale ratios. The relation between the power-law index and the critical buckling temperature for these sandwich plates is similar to what is observed in vibration behaviours.

**5. Conclusions**

In this study, general quasi-3D and higher-order shear deformation models are developed to study the mechanical and thermal behaviours of FG sandwich microplates. Governing equations are derived from the variational principle based on the framework of the modified couple stress theory. The Navier solutions are applied to examine the bending, vibration and buckling behaviours of microplates under mechanical and thermal loads. These solutions reveal that the inclusion of small-scale effect increases the microplates' stiffness, especially for those with the thickness $h < 20l$ . In addition, comprising thickness stretching strain in mechanical analysis results in higher stiffness for FG plates which leads to smaller deflection and higher natural frequencies as well as critical buckling loads, compared with the higher-order 2D models. Moreover, thickness stretching thermal strain also induces the out-of-plane thermal load in the thermal analysis which leads to the higher deflections, stresses as well as lower natural frequency and critical buckling temperature.

## References

[1] Ilkhani MR, Hosseini-Hashemi SH. Size dependent vibro-buckling of rotating beam based on modified couple stress theory. Composite Structures. 2016;143:75-83.

[2] Cosserat E, Cosserat F. Theory of deformable bodies (Translated by D.H. Delphenich). Paris: Sorbonne: Herman and Sons; 1909.

[3] Mindlin RD. Second gradient of strain and surface tension in linear elasticity. Archive for Rational Mechanics and Analysis. 1965;16:51-78.

[4] Fleck NA, Hutchinson JW. A reformulation of strain gradient plasticity. Journal of the Mechanics and Physics of Solids. 2001;49:2245-71.

[5] Lam DCC, Yang F, Chong ACM, Wang J, Tong P. Experiments and theory in strain gradient elasticity. Journal of the Mechanics and Physics of Solids. 2003;51(8):1477-508.

[6] Eringen AC. On differential equations of nonlocal elasticity and solutions of screw dislocation and surface waves. Journal of Applied Physics. 1983;54:4703-10.

[7] Reddy JN, El-Borgi S, Romanoff J. Non-linear analysis of functionally graded microbeams using Eringen′s non-local differential model. International Journal of Non-Linear Mechanics. 2014;67:308-18.

[8] Apuzzo A, Barretta R, Canadija M, Feo L, Luciano R, Marotti de Sciarra F. A closed-form model for torsion of nanobeams with an enhanced nonlocal formulation. Composites Part B: Engineering. 2017;108:315-24.

[9] Barretta R, Feo L, Luciano R, Marotti de Sciarra F. Application of an enhanced version of the Eringen differential model to nanotechnology. Composites Part B: Engineering. 2016;96:274-80.

[10] Barretta R, Feo L, Luciano R, Marotti de Sciarra F, Penna R. Functionally graded Timoshenko nanobeams: A novel nonlocal gradient formulation. Composites Part B: Engineering. 2016;100:208-19.

[11] Romano G, Barretta R, Diaco M. Micromorphic continua: non-redundant formulations. Continuum Mechanics and Thermodynamics. 2016;28(6):1659-70.

[12] Yang F, Chong ACM, Lam DCC, Tong P. Couple stress based strain gradient theory for elasticity. International Journal of Solids and Structures. 2002;39:2731–43.

[13] Akgöz B, Civalek Ö. Strain gradient elasticity and modified couple stress models for buckling analysis of axially loaded micro-scaled beams. International Journal of Engineering Science. 2011;49(11):1268-80.

[14] Hadjesfandiari AR, Dargush GF. Couple stress theory for solids. International Journal of Solids and Structures. 2011;48(18):2496-510.

[15] Ke LL, Yang J, Kitipornchai S, Bradford MA. Bending, buckling and vibration of size-dependent functionally graded annular microplates. Composite Structures. 2012;94(11):3250-7.

[16] Asghari M, Taati E. A size-dependent model for functionally graded micro-plates for mechanical analyses. Journal of Vibration and Control. 2012;19(11):1614-32.

[17] Taati E. Analytical solutions for the size dependent buckling and postbuckling behavior of functionally graded micro-plates. International Journal of Engineering Science. 2016;100:45-60.

[18] Thai H-T, Choi D-H. Size-dependent functionally graded Kirchhoff and Mindlin plate models based on a modified couple stress theory. Composite Structures. 2013;95:142-53.

[19] Jung W-Y, Han S-C, Park W-T. A modified couple stress theory for buckling analysis of S-FGM nanoplates embedded in Pasternak elastic medium. Composites Part B: Engineering. 2014;60:746-56.

[20] Jung W-Y, Park W-T, Han S-C. Bending and vibration analysis of S-FGM microplates embedded in Pasternak elastic medium using the modified couple stress theory. International Journal of Mechanical Sciences. 2014;87:150-62.

[21] Ansari R, Faghih Shojaei M, Mohammadi V, Gholami R, Darabi MA. Nonlinear vibrations of functionally graded Mindlin microplates based on the modified couple stress theory. Composite Structures. 2014;114:124-34.

[22] Ansari R, Gholami R, Faghih Shojaei M, Mohammadi V, Darabi MA. Size-dependent nonlinear bending and postbuckling of functionally graded Mindlin rectangular microplates considering the physical neutral plane position. Composite Structures. 2015;127:87-98.

[23] Thai H-T, Kim S-E. A size-dependent functionally graded Reddy plate model based on a modified couple stress theory. Composites Part B: Engineering. 2013;45(1):1636-45.

[24] Eshraghi I, Dag S, Soltani N. Consideration of spatial variation of the length scale parameter in static and dynamic analyses of functionally graded annular and circular micro-plates. Composites Part B: Engineering. 2015;78:338-48.

[25] Thai H-T, Vo TP. A size-dependent functionally graded sinusoidal plate model based on a modified couple stress theory. Composite Structures. 2013;96:376-83.

[26] He L, Lou J, Zhang E, Wang Y, Bai Y. A size-dependent four variable refined plate model for functionally graded microplates based on modified couple stress theory. Composite Structures. 2015;130:107-15.

[27] Lou J, He LW, Du JK. A unified higher order plate theory for functionally graded microplates based on the modified couple stress theory. Composite Structures. 2015;133:1036-47.

[28] Nguyen HX, Nguyen TN, Abdel-Wahab M, Bordas SPA, Nguyen-Xuan H, Vo TP. A refined quasi-3D isogeometric analysis for functionally graded microplates based on the modified couple stress theory. Computer Methods in Applied Mechanics and Engineering. 2017;313:904-40.

[29] Reddy JN, Kim J. A nonlinear modified couple stress-based third-order theory of functionally graded plates. Composite Structures. 2012;94(3):1128-43.

[30] Kim J, Reddy JN. Analytical solutions for bending, vibration, and buckling of FGM plates using a couple stress-based third-order theory. Composite Structures. 2013;103:86-98.

[31] Mirsalehi M, Azhari M, Amoushahi H. Stability of thin FGM microplate subjected to mechanical and thermal loading based on the modified couple stress theory and spline finite strip method. Aerospace Science and Technology. 2015;47:356-66.

[32] Ashoori AR, Sadough Vanini SA. Thermal buckling of annular microstructure-dependent functionally graded material plates resting on an elastic medium. Composites Part B: Engineering. 2016;87:245-55.

[33] Eshraghi I, Dag S, Soltani N. Bending and free vibrations of functionally graded annular and circular micro-plates under thermal loading. Composite Structures. 2016;137:196-207.

[34] Touloukian YS. Thermophysical properties of high temperature solid materials. Newyork: Macmillan; 1967.

[35] Zenkour AM, Alghamdi NA. Thermoelastic bending analysis of functionally graded sandwich plates. Journal of Materials Science. 2008;43(8):2574-89.

[36] Thai H-T, Kim S-E. A simple quasi-3D sinusoidal shear deformation theory for functionally graded plates. Composite Structures. 2013;99:172-80.

[37] Vo TP, Thai H-T, Nguyen T-K, Inam F, Lee J. A quasi-3D theory for vibration and buckling of functionally graded sandwich beams. Composite Structures. 2015;119:1-12.

[38] Lei J, He Y, Zhang B, Liu D, Shen L, Guo S. A size-dependent FG micro-plate model incorporating higher-order shear and normal deformation effects based on a modified couple stress theory. International Journal of Mechanical Sciences. 2015;104:8-23.

[39] Tounsi A, Houari MSA, Benyoucef S, Adda Bedia EA. A refined trigonometric shear deformation theory for thermoelastic bending of functionally graded sandwich plates. Aerospace Science and Technology. 2013;24(1):209-20.

[40] Mantari JL, Granados EV. Thermoelastic analysis of advanced sandwich plates based on a new quasi-3D hybrid type HSDT with 5 unknowns. Composites Part B: Engineering. 2015;69:317-34.

[41] Ungbhakorn V, Wattanasakulpong N. Thermo-elastic vibration analysis of third-order shear deformable functionally graded plates with distributed patch mass under thermal environment. Applied Acoustics. 2013;74(9):1045-59.

[42] Bouiadjra MB, Ahmed Houari MS, Tounsi A. Thermal Buckling of Functionally Graded Plates According to a Four-Variable Refined Plate Theory. Journal of Thermal Stresses. 2012;35(8):677-94.

[43] Akavci SS. Thermal Buckling Analysis of Functionally Graded Plates on an Elastic Foundation According to a Hyperbolic Shear Deformation Theory. Mech Compos Mater. 2014;50(2):197-212.

## APPENDIX

$$N_{xx}=A_{11}\frac{\partial U}{\partial x}+A_{12}\frac{\partial V}{\partial y}-B_{11}\frac{\partial^2 W_b}{\partial x^2}-B_{12}\frac{\partial^2 W_b}{\partial y^2}-B_{11}^s\frac{\partial^2 W_s}{\partial x^2}-B_{12}^s\frac{\partial^2 W_s}{\partial y^2}+K_{13}W_z-\left(A_t\Delta T_1+B_t\frac{\Delta T_2}{h}\right) \quad \text{(A1)}$$

$$N_{yy}=A_{12}\frac{\partial U}{\partial x}+A_{22}\frac{\partial V}{\partial y}-B_{12}\frac{\partial^2 W_b}{\partial x^2}-B_{22}\frac{\partial^2 W_b}{\partial y^2}-B_{12}^s\frac{\partial^2 W_s}{\partial x^2}-B_{22}^s\frac{\partial^2 W_s}{\partial y^2}+K_{23}W_z-\left(A_t\Delta T_1+B_t\frac{\Delta T_2}{h}\right) \quad \text{(A2)}$$

$$N_{xy}=A_{66}\left(\frac{\partial U}{\partial y}+\frac{\partial V}{\partial x}\right)-2B_{66}\frac{\partial^2 W_b}{\partial x\partial y}-2B_{66}^s\frac{\partial^2 W_s}{\partial x\partial y} \quad \text{(A3)}$$

$$M_{xx}=B_{11}\frac{\partial U}{\partial x}+B_{12}\frac{\partial V}{\partial y}-D_{11}\frac{\partial^2 W_b}{\partial x^2}-D_{12}\frac{\partial^2 W_b}{\partial y^2}-D_{11}^s\frac{\partial^2 W_s}{\partial x^2}-D_{12}^s\frac{\partial^2 W_s}{\partial y^2}+L_{13}W_z-\left(B_t\Delta T_1+D_t\frac{\Delta T_2}{h}\right) \quad \text{(A4)}$$

$$M_{yy}=B_{12}\frac{\partial U}{\partial x}+B_{22}\frac{\partial V}{\partial y}-D_{12}\frac{\partial^2 W_b}{\partial x^2}-D_{22}\frac{\partial^2 W_b}{\partial y^2}-D_{12}^s\frac{\partial^2 W_s}{\partial x^2}-D_{22}^s\frac{\partial^2 W_s}{\partial y^2}+L_{23}W_z-\left(B_t\Delta T_1+D_t\frac{\Delta T_2}{h}\right) \quad \text{(A5)}$$

$$M_{xy}=B_{66}\left(\frac{\partial U}{\partial y}+\frac{\partial V}{\partial x}\right)-2D_{66}\frac{\partial^2 W_b}{\partial x\partial y}-2D_{66}^s\frac{\partial^2 W_s}{\partial x\partial y} \quad \text{(A6)}$$

$$P_{xx}=B_{11}^s\frac{\partial U}{\partial x}+B_{12}^s\frac{\partial V}{\partial y}-D_{11}^s\frac{\partial^2 W_b}{\partial x^2}-D_{12}^s\frac{\partial^2 W_b}{\partial y^2}-H_{11}\frac{\partial^2 W_s}{\partial x^2}-H_{12}\frac{\partial^2 W_s}{\partial y^2}+L_{13}^sW_z-\left(B_t^s\Delta T_1+D_t^s\frac{\Delta T_2}{h}\right) \quad \text{(A7)}$$

$$P_{yy}=B_{12}^s\frac{\partial U}{\partial x}+B_{22}^s\frac{\partial V}{\partial y}-D_{12}^s\frac{\partial^2 W_b}{\partial x^2}-D_{22}^s\frac{\partial^2 W_b}{\partial y^2}-H_{12}\frac{\partial^2 W_s}{\partial x^2}-H_{22}\frac{\partial^2 W_s}{\partial y^2}+L_{23}^sW_z-\left(B_t^s\Delta T_1+D_t^s\frac{\Delta T_2}{h}\right) \quad \text{(A8)}$$

$$P_{xy}=B_{66}^s\left(\frac{\partial U}{\partial y}+\frac{\partial V}{\partial x}\right)-2D_{66}^s\frac{\partial^2 W_b}{\partial x\partial y}-2H_{66}\frac{\partial^2 W_s}{\partial x\partial y} \quad \text{(A9)}$$

$$O_{zz}=K_{13}\frac{\partial U}{\partial x}+K_{23}\frac{\partial V}{\partial y}-L_{13}\frac{\partial^2 W_b}{\partial x^2}-L_{23}\frac{\partial^2 W_b}{\partial y^2}-L_{13}^s\frac{\partial^2 W_s}{\partial x^2}-L_{23}^s\frac{\partial^2 W_s}{\partial y^2}+Z_{33}W_z-\left(C_t\Delta T_1+C_t^s\frac{\Delta T_2}{h}\right) \quad \text{(A10)}$$

$$Q_{xz}=A_{55}^s\left(\frac{\partial W_s}{\partial x}+\frac{\partial W_z}{\partial x}\right) \quad \text{(A11)}$$

$$Q_{yz}=A_{44}^s\left(\frac{\partial W_s}{\partial y}+\frac{\partial W_z}{\partial y}\right) \quad \text{(A12)}$$

$$R_{xx}=2A_m\frac{\partial^2 W_b}{\partial x\partial y}+\left(A_m+B_m\right)\frac{\partial^2 W_s}{\partial x\partial y}+E_m\frac{\partial^2 W_z}{\partial x\partial y} \quad \text{(A13)}$$

$$R_{yy}=-2A_m\frac{\partial^2 W_b}{\partial x\partial y}-\left(A_m+B_m\right)\frac{\partial^2 W_s}{\partial x\partial y}-E_m\frac{\partial^2 W_z}{\partial x\partial y} \quad \text{(A14)}$$

$$R_{xy}=A_m\frac{\partial^2 W_b}{\partial y^2}+\frac{1}{2}\left(A_m+B_m\right)\frac{\partial^2 W_s}{\partial y^2}+\frac{1}{2}E_m\frac{\partial^2 W_z}{\partial y^2}-A_m\frac{\partial^2 W_b}{\partial x^2}-\frac{1}{2}\left(A_m+B_m\right)\frac{\partial^2 W_s}{\partial x^2}-\frac{1}{2}E_m\frac{\partial^2 W_z}{\partial x^2} \quad \text{(A15)}$$

$$R_{xz} = \frac{1}{2} A_m \frac{\partial^2 V}{\partial x^2} - \frac{1}{2} A_m \frac{\partial^2 U}{\partial x \partial y} - \frac{1}{2} G_m \frac{\partial W_s}{\partial y} + \frac{1}{2} G_m \frac{\partial W_z}{\partial y} \tag{A16}$$

$$R_{yz} = \frac{1}{2} A_m \frac{\partial^2 V}{\partial x \partial y} - \frac{1}{2} A_m \frac{\partial^2 U}{\partial y^2} + \frac{1}{2} G_m \frac{\partial W_s}{\partial x} - \frac{1}{2} G_m \frac{\partial W_z}{\partial x} \tag{A17}$$

$$S_{xx} = 2B_m \frac{\partial^2 W_b}{\partial x \partial y} + \left(B_m + C_m\right) \frac{\partial^2 W_s}{\partial x \partial y} + D_m \frac{\partial^2 W_z}{\partial x \partial y} \tag{A18}$$

$$S_{yy} = -2B_m \frac{\partial^2 W_b}{\partial x \partial y} - \left(B_m + C_m\right) \frac{\partial^2 W_s}{\partial x \partial y} - D_m \frac{\partial^2 W_z}{\partial x \partial y} \tag{A19}$$

$$S_{xy} = B_m \frac{\partial^2 W_b}{\partial y^2} + \frac{1}{2}\left(B_m + C_m\right) \frac{\partial^2 W_s}{\partial y^2} + \frac{1}{2} D_m \frac{\partial^2 W_z}{\partial y^2} - B_m \frac{\partial^2 W_b}{\partial x^2} - \frac{1}{2}\left(B_m + C_m\right) \frac{\partial^2 W_s}{\partial x^2} - \frac{1}{2} D_m \frac{\partial^2 W_z}{\partial x^2} \tag{A20}$$

$$T_{xx} = 2E_m \frac{\partial^2 W_b}{\partial x \partial y} + \left(E_m + D_m\right) \frac{\partial^2 W_s}{\partial x \partial y} + F_m \frac{\partial^2 W_z}{\partial x \partial y} \tag{A21}$$

$$T_{yy} = -2E_m \frac{\partial^2 W_b}{\partial x \partial y} - \left(E_m + D_m\right) \frac{\partial^2 W_s}{\partial x \partial y} - F_m \frac{\partial^2 W_z}{\partial x \partial y} \tag{A22}$$

$$T_{xy} = E_m \frac{\partial^2 W_b}{\partial y^2} + \frac{1}{2}\left(E_m + D_m\right) \frac{\partial^2 W_s}{\partial y^2} + \frac{1}{2} F_m \frac{\partial^2 W_z}{\partial y^2} - E_m \frac{\partial^2 W_b}{\partial x^2} - \frac{1}{2}\left(E_m + D_m\right) \frac{\partial^2 W_s}{\partial x^2} - \frac{1}{2} F_m \frac{\partial^2 W_z}{\partial x^2} \tag{A23}$$

$$X_{xz} = -\frac{1}{2} G_m \frac{\partial^2 V}{\partial x^2} + \frac{1}{2} G_m \frac{\partial^2 U}{\partial x \partial y} + \frac{1}{2} H_m \frac{\partial W_s}{\partial y} - \frac{1}{2} H_m \frac{\partial W_z}{\partial y} \tag{A24}$$

$$X_{yz} = -\frac{1}{2} G_m \frac{\partial^2 V}{\partial x \partial y} + \frac{1}{2} G_m \frac{\partial^2 U}{\partial y^2} - \frac{1}{2} H_m \frac{\partial W_s}{\partial x} + \frac{1}{2} H_m \frac{\partial W_z}{\partial x} \tag{A25}$$

where

$$\left(A_{ij}, A_{ij}^s, B_{ij}, B_{ij}^s, D_{ij}, D_{ij}^s, H_{ij}\right) = \int_{-h/2}^{h/2} \left[1, g^2(z), z, f(z), z^2, f(z) z, f^2(z)\right] Q_{ij} dz \tag{A26}$$

$$\left(K_{ij}, L_{ij}, L_{ij}^s, Z_{ij}\right) = \int_{-h/2}^{h/2} \left[1, z, f(z), \frac{\partial g(z)}{\partial z}\right] \frac{\partial g(z)}{\partial z} Q_{ij} dz \tag{A27}$$

$$\begin{aligned}&\left(A_m, B_m, C_m, D_m, E_m, F_m, G_m, H_m\right) \\ &= \int_{-h/2}^{h/2} l^2 \mu \left(1, \frac{\partial f(z)}{\partial z}, \left[\frac{\partial f(z)}{\partial z}\right]^2, \frac{\partial f(z)}{\partial z} g(z), g(z), \left[g(z)\right]^2, \frac{\partial g(z)}{\partial z}, \left[\frac{\partial g(z)}{\partial z}\right]^2\right) dz\end{aligned} \tag{A28}$$

$$A_t = \int_{-h/2}^{h/2} \alpha(z,T)\left(Q_{11} + 2Q_{12}\right) dz \;;\; B_t = \int_{-h/2}^{h/2} \alpha(z,T)\left(Q_{11} + 2Q_{12}\right) z dz\;; \tag{A29}$$

$$B_t^s = \int_{-h/2}^{h/2} \alpha\left(z,T\right)\left(Q_{11}+2Q_{12}\right)f\left(z\right)dz\,;C_t = \int_{-h/2}^{h/2} \alpha\left(z,T\right)\left(Q_{11}+2Q_{12}\right)\frac{d^2 f}{dz^2}dz\,; \tag{A30}$$

$$C_t^s = \int_{-h/2}^{h/2} \alpha\left(z,T\right)\left(Q_{11}+2Q_{12}\right)\frac{d^2 f}{dz^2}zdz\,;D_t = \int_{-h/2}^{h/2} \alpha\left(z,T\right)\left(Q_{11}+2Q_{12}\right)z^2 dz\,; \tag{A31}$$

$$D_t^s = \int_{-h/2}^{h/2} \alpha\left(z,T\right)\left(Q_{11}+2Q_{12}\right)f\left(z\right)zdz \tag{A32}$$

## LIST OF FIGURES

## LIST OF TABLES

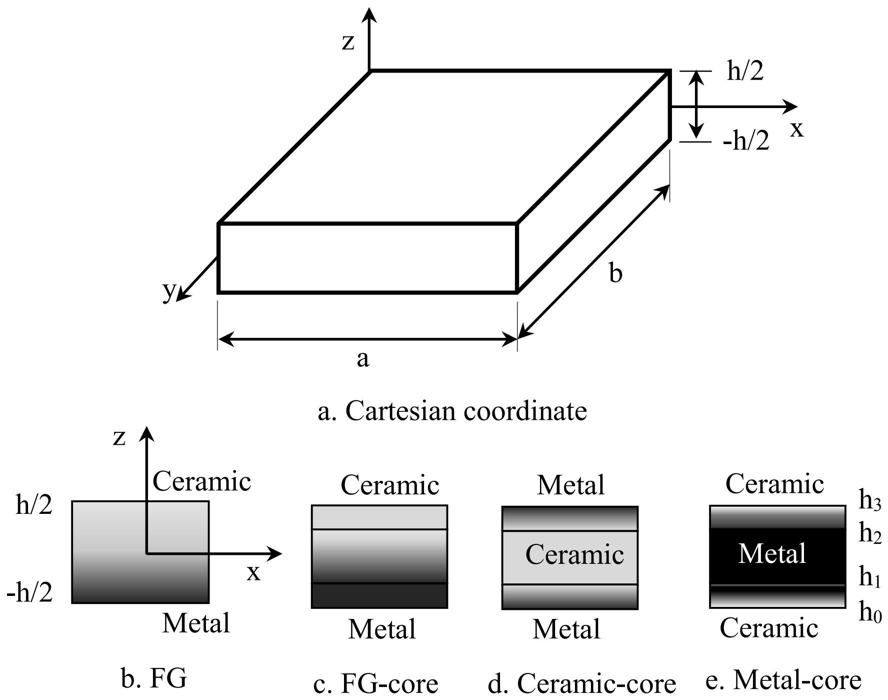


Fig. 1: Coordinate and cross-section of FG/FG sandwich plates.

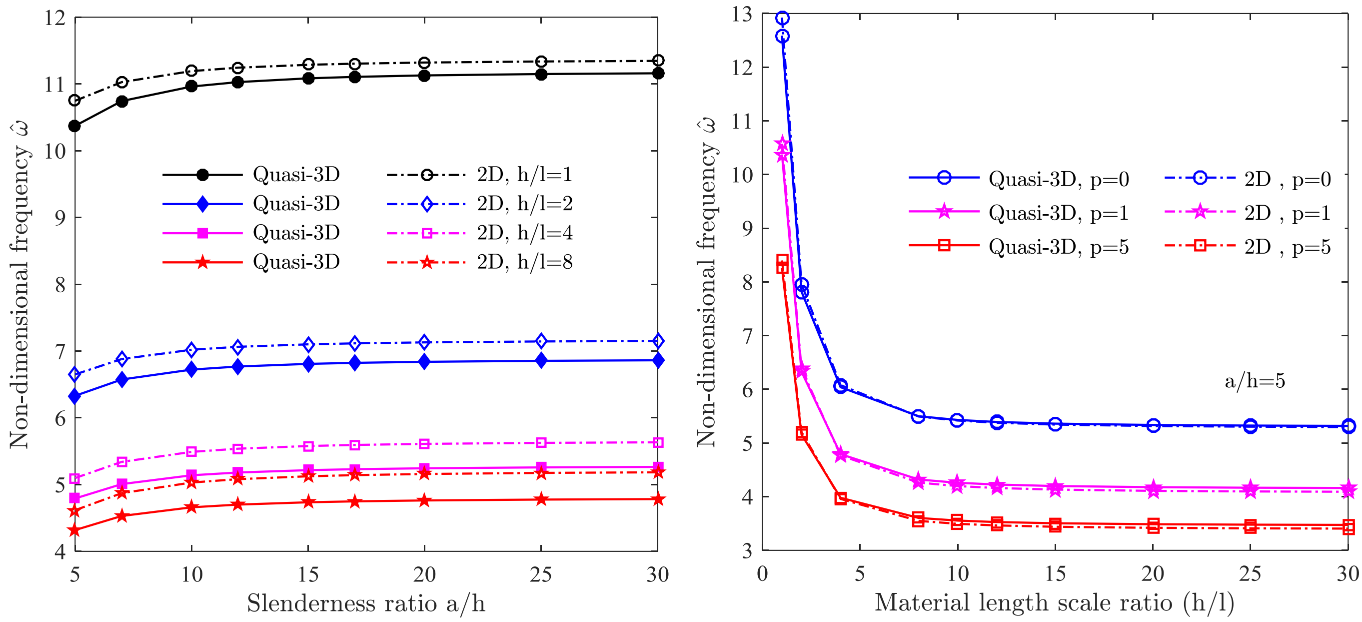


Fig. 2: Non-dimensional frequencies of $Al/Al_2O_3$ microplates with various slenderness and material length scale ratios.

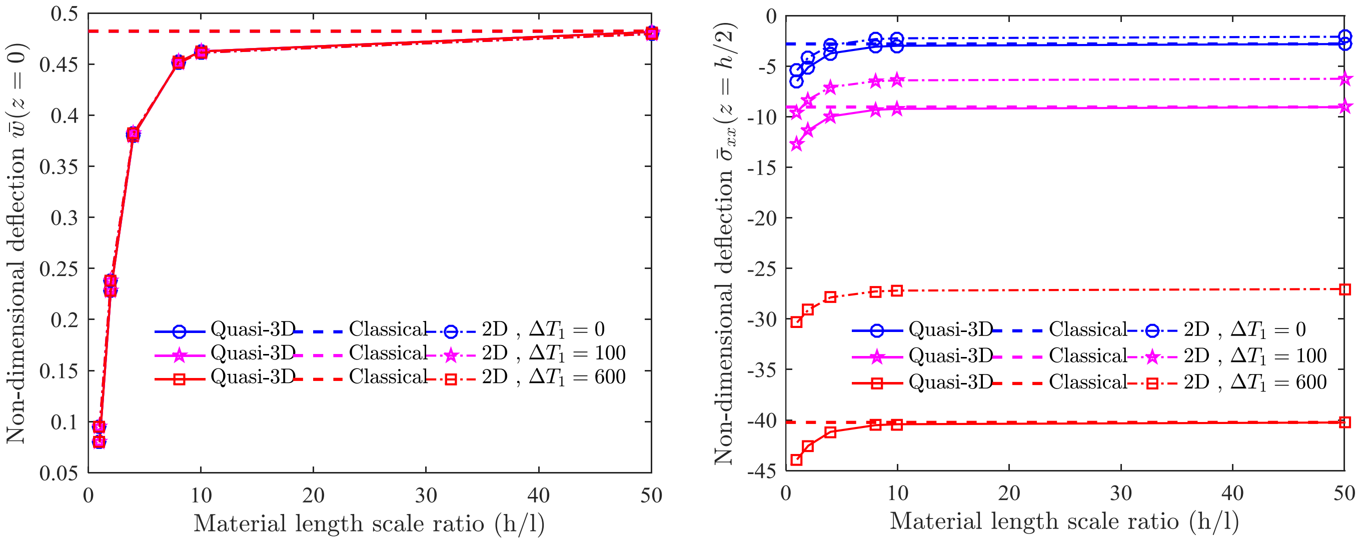


a) p = 0

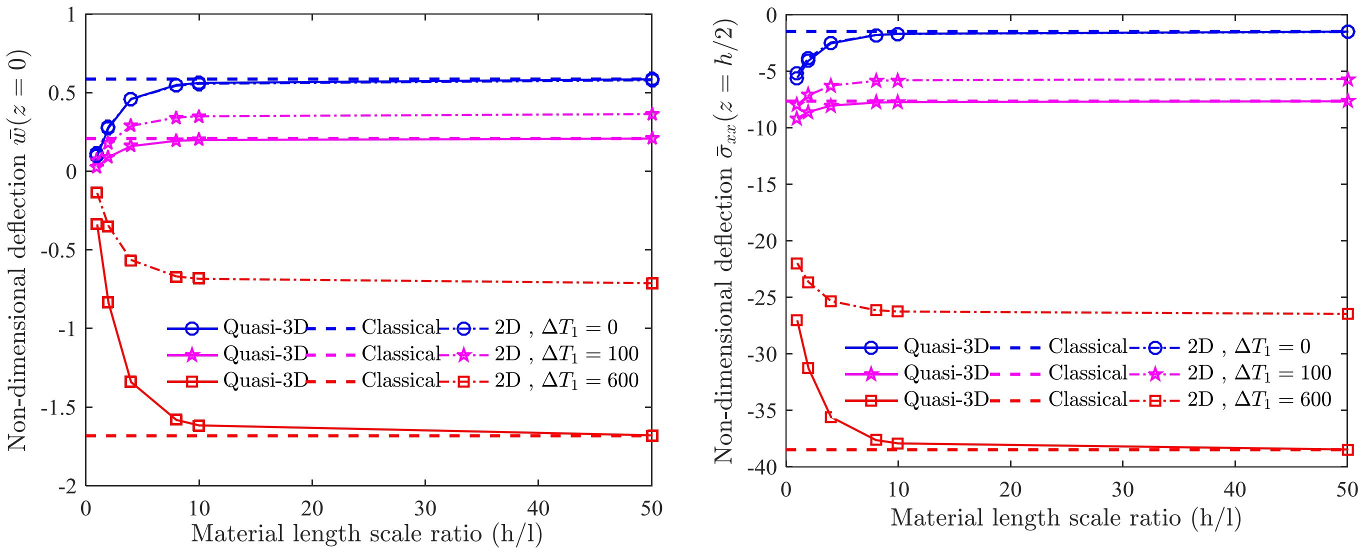


b) p = 1

Fig. 3: Non-dimensional deflections and stresses of Ti-6Al-4V/$ZrO_2$ microplates for various material length scale ratios and temperatures.

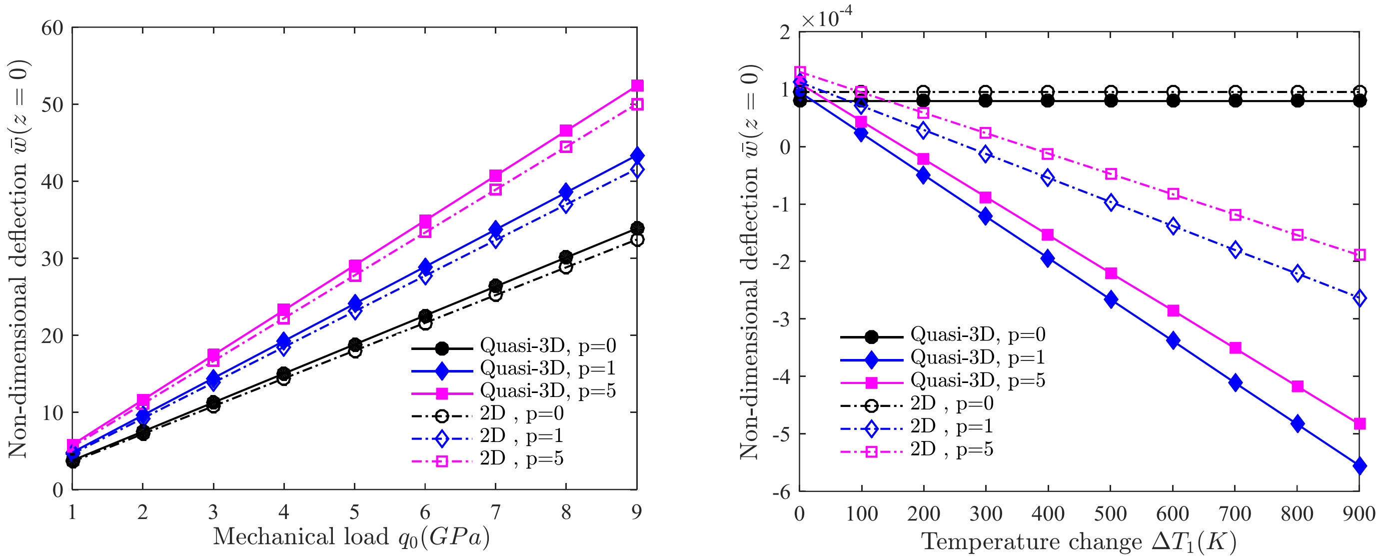


a) h/l=1

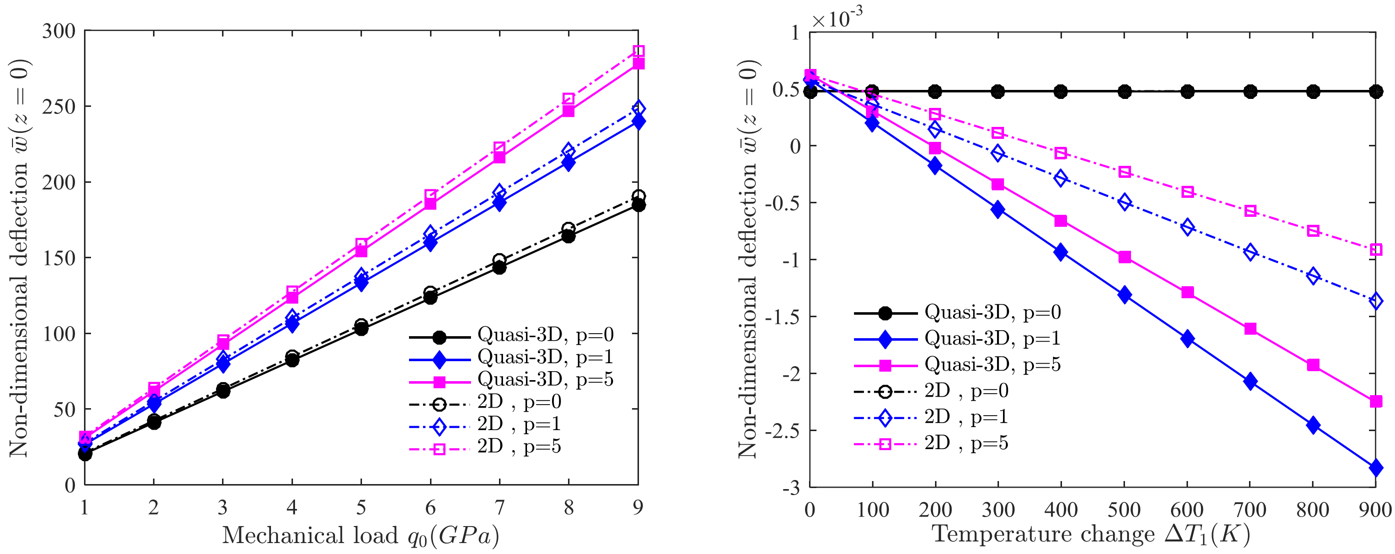


b) Classical

Fig. 4: Non-dimensional deflections of Ti-6Al-4V/ZrO2 microplates under various mechanical and thermal loads.

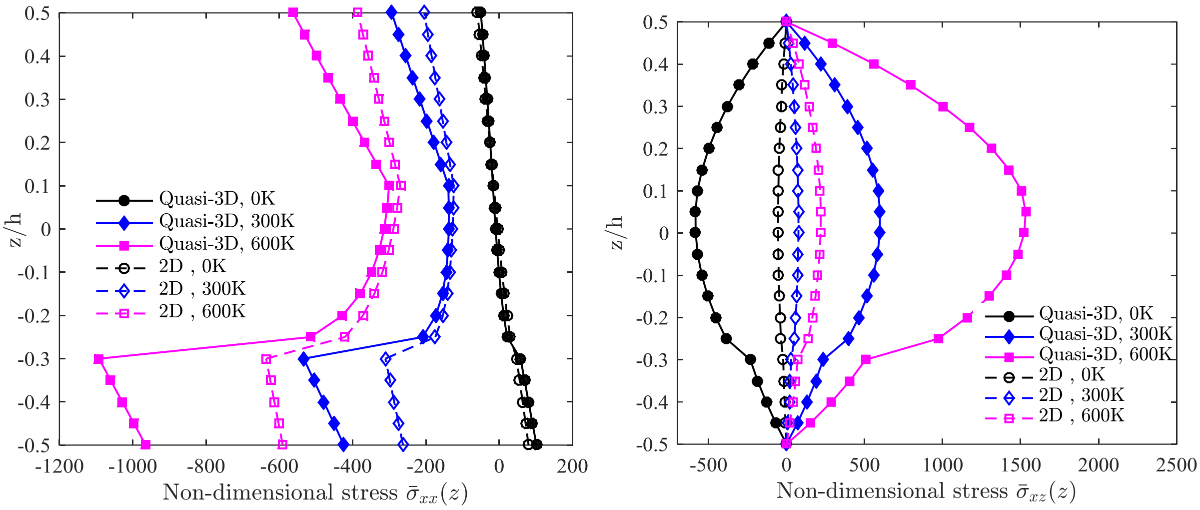


a. FG-core sandwich plates

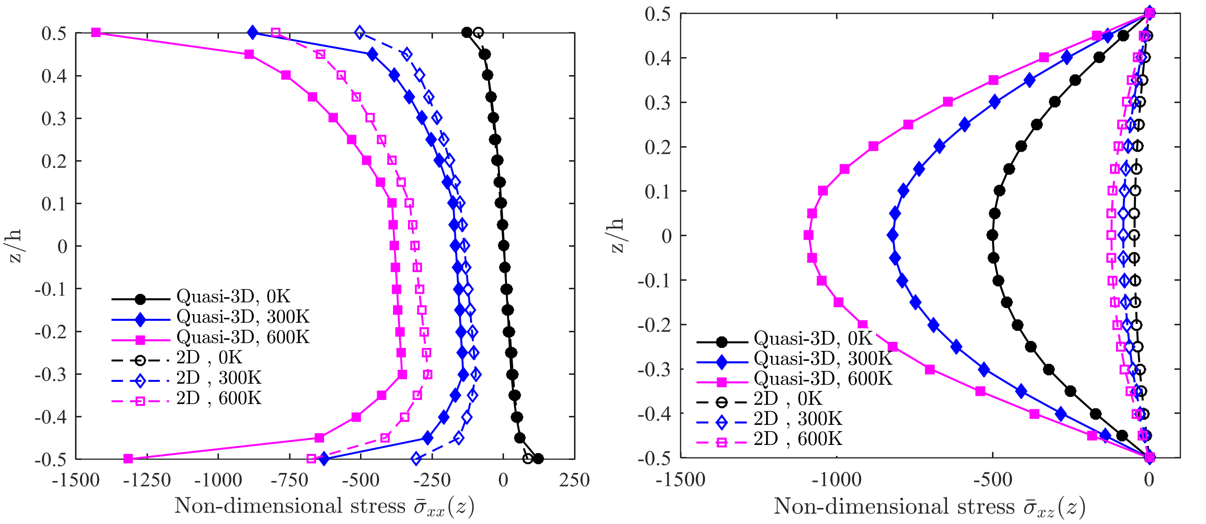


b. Ceramic-core sandwich plates

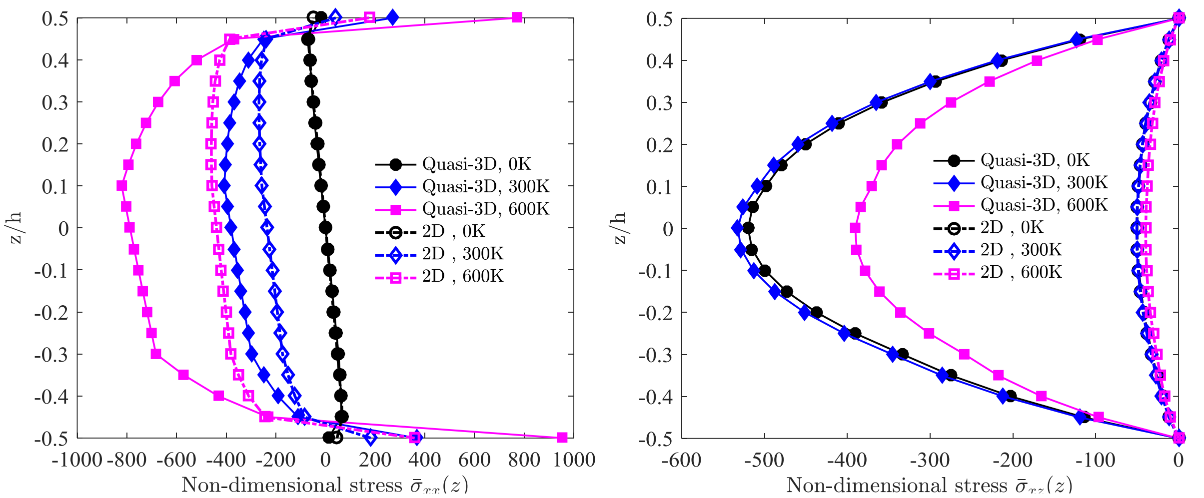


c. Metal-core sandwich plates

Fig. 5: Distribution of non-dimensional stresses of (1-2-2) $Si_3N_4$/SUS304 microplates through the thickness under various linear temperatures (h/l=1, p=0.2).

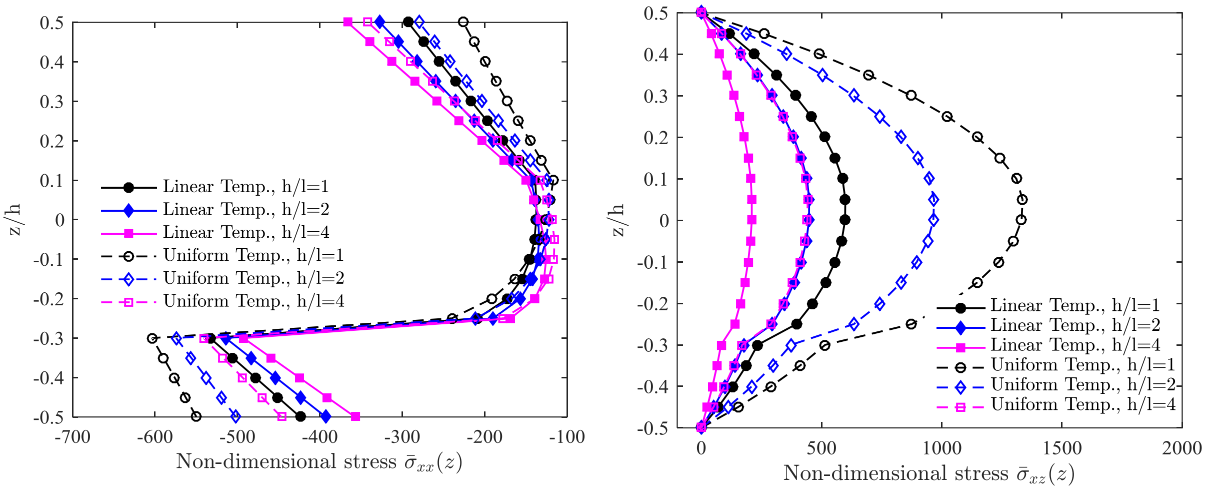


a. FG-core sandwich plates

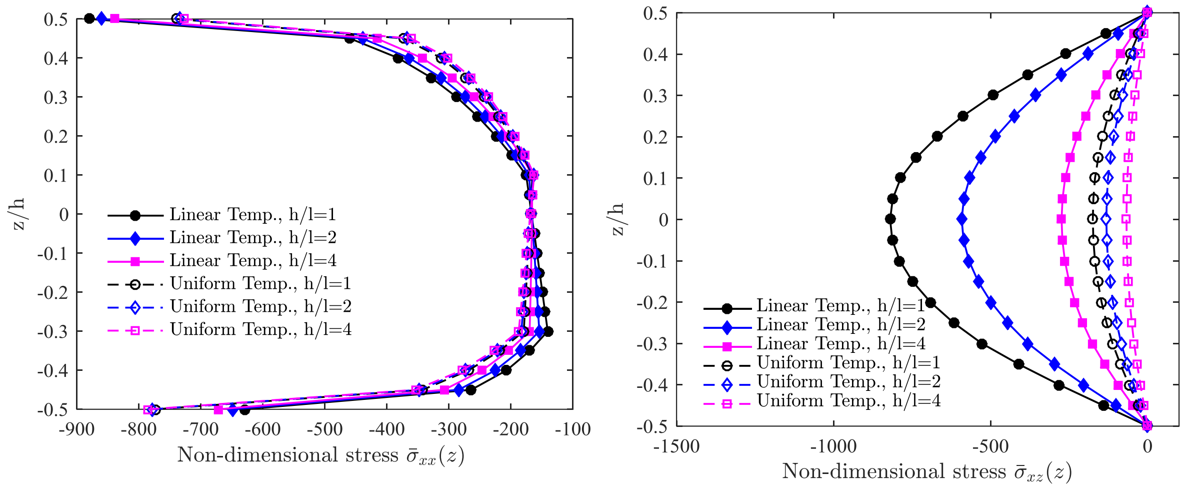


b. Ceramic-core sandwich plates

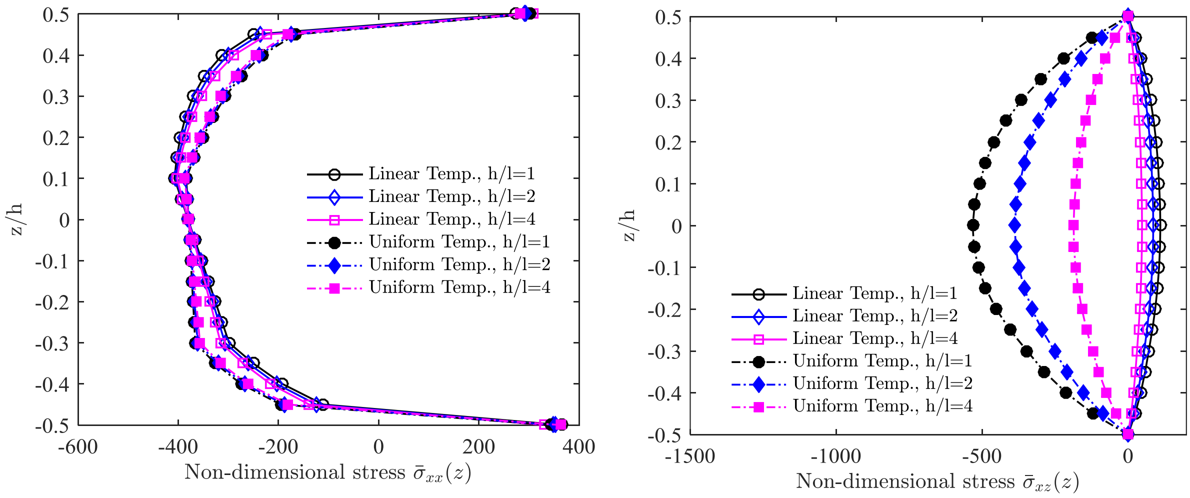


c. Metal-core sandwich plates

Fig. 6: Distribution of non-dimensional stresses of (1-2-2) $Si_3N_4$/SUS304 microplates through the thickness for various material length scale ratios (p=0.2, $\Delta T_1$ = 300K).

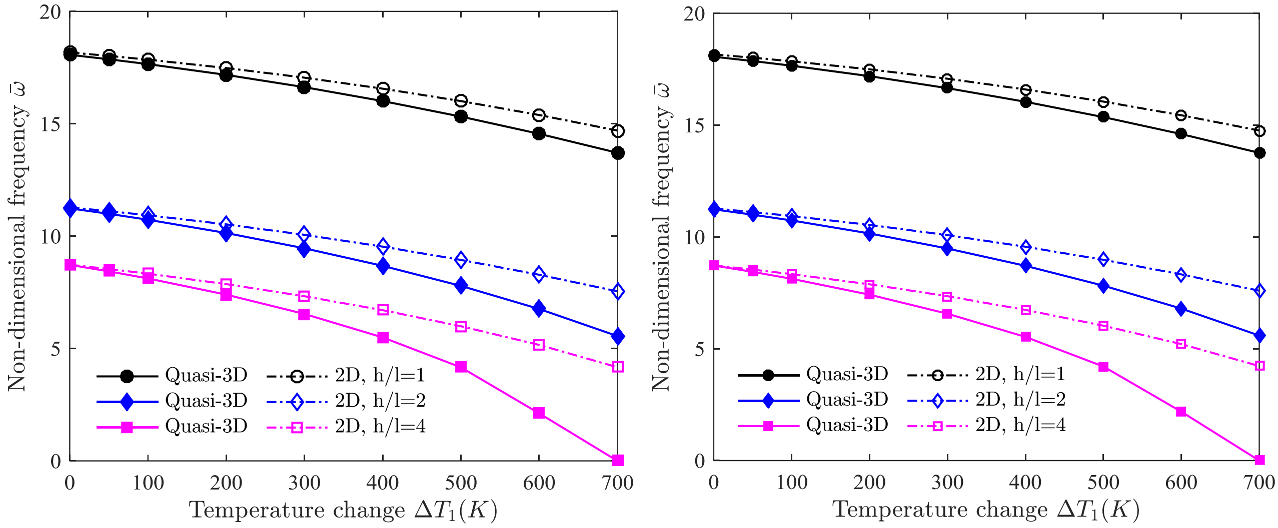


a. Uniform temperature

b. Linear temperature

Fig. 7: Non-dimensional frequencies of $Si_3N_4$/SUS304 microplates for various material length scale ratios under uniform and linear temperatures.

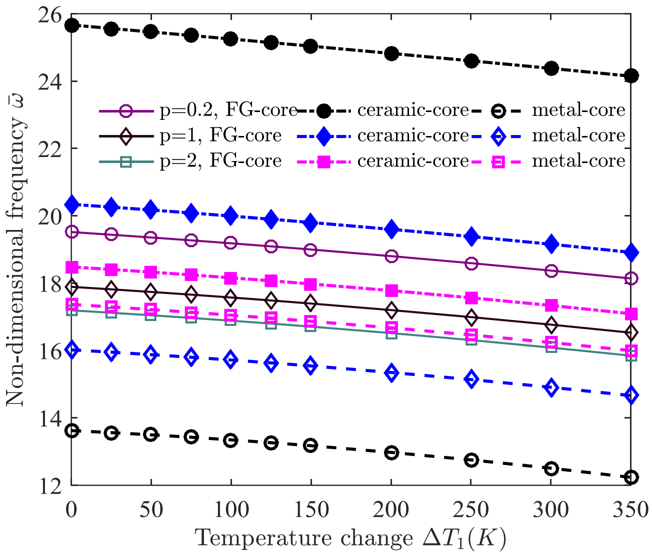


a. Uniform

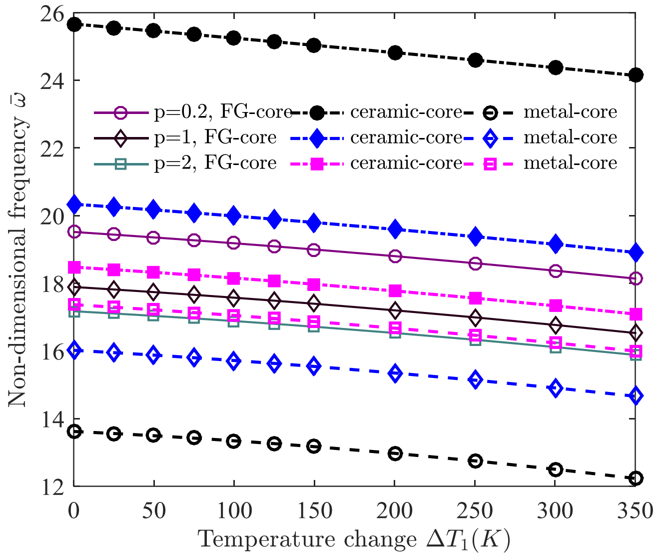


b. Linear

Fig. 8: Non-dimensional frequencies of (1-1-1) $Si_3N_4$/SUS304 microplates for various power-law index under uniform and linear temperature (h/l=1).

Table 1: Material properties of FG plates for mechanical and temperature-independent (TID) thermal analysis.

| Material | | Material properties | | |
|---|---|---|---|---|
| | | E (GPa) | α (1/K) | ν |
| Metal: | Ti–6A1–4V | 66.2 | 10.3e-6 | 1/3 |
| | Al | 70 | - | 0.3 |
| | $Mat_1$ | 14.4 | - | 0.38 |
| Ceramic: | $ZrO_2$ | 117 | 7.11e-6 | 1/3 |
| | $Al_2O_3$ | 380 | - | 0.3 |
| | $Mat_2$ | 1.44 | - | 0.38 |

Table 2: Temperature-dependent coefficients of $Si_3N_4$/SUS304 plates.

| Materials | Proprieties | $P_0$ | $P_{-1}$ | $P_1$ | $P_2$ | $P_3$ |
|---|---|---|---|---|---|---|
| $Si_3N_4$ | E (Pa) | 348.43e+9 | 0.0 | −3.070e−4 | 2.160e−7 | −8.946e−11 |
| | α (1/K) | 5.8723e−6 | 0.0 | 9.095e−4 | 0.0 | 0.0 |
| | κ (W/mK) | 13.723 | 0.0 | −1.032e−3 | 5.466e−7 | −7.876e−11 |
| | ν | 0.24 | 0.0 | 0.0 | 0.0 | 0.0 |
| | ρ ($kg/m^3$) | 2370 | 0.0 | 0.0 | 0.0 | 0.0 |
| SUS304 | E (Pa) | 201.04e+9 | 0.0 | 3.079e−4 | −6.534e−7 | 0.0 |
| | α (1/K) | 12.330e−6 | 0.0 | 8.086e−4 | 0.0 | 0.0 |
| | κ (W/mK) | 15.379 | 0.0 | −1.264e−3 | 2.092e−6 | −7.223e−10 |
| | ν | 0.3262 | 0.0 | −2.002e−4 | 3.797e−7 | 0.0 |
| | ρ ($kg/m^3$) | 8166 | 0.0 | 0.0 | 0.0 | 0.0 |

Table 3: Non-dimensional deflections and stresses of $Al/Al_2O_3$ microplates under sinusoidal loads.

| a/h | h/l | Theory | $\bar{w}(a/2,b/2,0)$ | | | $\bar{\sigma}_{xx}(a/2,b/2,h/2)$ | | |
|---|---|---|---|---|---|---|---|---|
| | | | p=0 | 1 | 10 | p=0 | 1 | 10 |
| 5 | 1 | TSDT [38] | 0.0569 | 0.0989 | 0.2077 | 0.2321 | 0.3162 | 0.6655 |
| | | SSDT [25] | 0.0588 | 0.1017 | 0.2158 | 0.1800 | 0.2437 | 0.5189 |
| | | Present TSDT | 0.0568 | 0.0985 | 0.2099 | 0.1841 | 0.2483 | 0.5294 |
| | | Present SSDT | 0.0570 | 0.0988 | 0.2108 | 0.1844 | 0.2488 | 0.5289 |
| | | Quasi-3D (TSDT) [38] | 0.0601 | 0.1031 | 0.2215 | 0.1878 | 0.2603 | 0.5232 |
| | | Present quasi-3D (TSDT) | 0.0587 | 0.1008 | 0.2171 | 0.1858 | 0.2562 | 0.5228 |
| | | Present quasi-3D (SSDT) | 0.0589 | 0.1012 | 0.2186 | 0.1968 | 0.2725 | 0.5531 |
| | 2 | TSDT [38] | 0.1432 | 0.2591 | 0.5113 | 0.5711 | 0.8185 | 1.5491 |
| | | Present TSDT | 0.1502 | 0.2715 | 0.5352 | 0.4729 | 0.6702 | 1.2939 |
| | | Present SSDT | 0.1506 | 0.2721 | 0.5387 | 0.4740 | 0.6720 | 1.2953 |
| | | Quasi-3D (TSDT) [38] | 0.1564 | 0.2781 | 0.5623 | 0.4888 | 0.7022 | 1.3087 |
| | | Present quasi-3D (TSDT) | 0.1533 | 0.2731 | 0.5468 | 0.4836 | 0.6930 | 1.2976 |
| | | Present quasi-3D (SSDT) | 0.1536 | 0.2736 | 0.5505 | 0.5117 | 0.7364 | 1.3733 |
| | 4 | TSDT [38] | 0.2316 | 0.4363 | 0.8275 | 0.9086 | 1.3660 | 2.3797 |
| | | Present TSDT | 0.2586 | 0.4881 | 0.9087 | 0.7891 | 1.1785 | 2.0694 |
| | | Present SSDT | 0.2589 | 0.4886 | 0.9141 | 0.7912 | 1.1818 | 2.0759 |
| | | Quasi-3D (TSDT) [38] | 0.2609 | 0.4827 | 0.9245 | 0.8156 | 1.2198 | 2.1200 |
| | | Present quasi-3D (TSDT) | 0.2583 | 0.4784 | 0.9039 | 0.8105 | 1.2112 | 2.0981 |
| | | Present quasi-3D (SSDT) | 0.2581 | 0.4781 | 0.9077 | 0.8543 | 1.2824 | 2.2117 |
| | 8 | TSDT [38] | 0.2740 | 0.5265 | 0.9865 | 1.0685 | 1.6427 | 2.7721 |
| | | Present TSDT | 0.3171 | 0.6118 | 1.1243 | 0.9529 | 1.4609 | 2.4657 |
| | | Present SSDT | 0.3172 | 0.6119 | 1.1275 | 0.9552 | 1.4648 | 2.4740 |
| | | Quasi-3D (TSDT) [38] | 0.3133 | 0.5916 | 1.1064 | 0.9793 | 1.4953 | 2.5197 |
| | | Present quasi-3D (TSDT) | 0.3123 | 0.5898 | 1.0963 | 0.9772 | 1.4917 | 2.5077 |
| | | Present quasi-3D (SSDT) | 0.3115 | 0.5886 | 1.0973 | 1.0276 | 1.5759 | 2.6329 |
| 10 | 1 | TSDT [38] | 0.0530 | 0.0926 | 0.1968 | 0.4836 | 0.6541 | 1.3774 |
| | | SSDT [25] | 0.0552 | 0.0959 | 0.2058 | 0.3749 | 0.5042 | 1.0733 |
| | | Present TSDT | 0.0546 | 0.0951 | 0.2043 | 0.3770 | 0.5065 | 1.0787 |
| | | Present SSDT | 0.0547 | 0.0951 | 0.2045 | 0.3771 | 0.5067 | 1.0785 |
| | | Quasi-3D (TSDT) [38] | 0.0556 | 0.0960 | 0.2066 | 0.3787 | 0.5184 | 1.0785 |
| | | Present quasi-3D (TSDT) | 0.0552 | 0.0954 | 0.2054 | 0.3778 | 0.5163 | 1.0785 |
| | | Present quasi-3D (SSDT) | 0.0552 | 0.0954 | 0.2057 | 0.4018 | 0.5520 | 1.1411 |
| | 2 | TSDT [38] | 0.1283 | 0.2355 | 0.4577 | 1.1622 | 1.6561 | 3.1516 |
| | | Present TSDT | 0.1401 | 0.2556 | 0.5022 | 0.9592 | 1.3542 | 2.6215 |
| | | Present SSDT | 0.1402 | 0.2558 | 0.5031 | 0.9598 | 1.3550 | 2.6222 |
| | | Quasi-3D (TSDT) [38] | 0.1419 | 0.2551 | 0.5050 | 0.9672 | 1.3775 | 2.6225 |
| | | Present quasi-3D (TSDT) | 0.1410 | 0.2537 | 0.5008 | 0.9646 | 1.3728 | 2.6170 |
| | | Present quasi-3D (SSDT) | 0.1410 | 0.2536 | 0.5015 | 1.0248 | 1.4665 | 2.7684 |
| | 4 | TSDT [38] | 0.1994 | 0.3837 | 0.6911 | 1.7954 | 2.6893 | 4.6805 |
| | | Present TSDT | 0.2313 | 0.4437 | 0.7998 | 1.5683 | 2.3352 | 4.1032 |
| | | Present SSDT | 0.2313 | 0.4438 | 0.8012 | 1.5694 | 2.3369 | 4.1066 |
| | | Quasi-3D (TSDT) [38] | 0.2320 | 0.4354 | 0.7933 | 1.5815 | 2.3517 | 4.0981 |
| | | Present quasi-3D (TSDT) | 0.2313 | 0.4343 | 0.7879 | 1.5790 | 2.3475 | 4.0871 |
| | | Present quasi-3D (SSDT) | 0.2308 | 0.4335 | 0.7885 | 1.6746 | 2.5036 | 4.3180 |
| | 8 | TSDT [38] | 0.2314 | 0.4554 | 0.7946 | 2.0799 | 3.1877 | 5.3392 |
| | | Present TSDT | 0.2766 | 0.5443 | 0.9455 | 1.8671 | 2.8552 | 4.7946 |
| | | Present SSDT | 0.2766 | 0.5443 | 0.9464 | 1.8683 | 2.8572 | 4.7988 |
| | | Quasi-3D (TSDT) [38] | 0.2757 | 0.5288 | 0.9265 | 1.8799 | 2.8567 | 4.7746 |
| | | Present quasi-3D (TSDT) | 0.2755 | 0.5284 | 0.9240 | 1.8789 | 2.8550 | 4.7687 |
| | | Present quasi-3D (SSDT) | 0.2747 | 0.5271 | 0.9237 | 1.9908 | 3.0421 | 5.0322 |

Table 4: Deflections and stresses of Ti-6Al-4V/$ZrO_2$ plates under xy-sinusoidal and z-linear temperature.

| p | Theory | z | $\bar{w}(a/2,b/2,z)$ | | | $\bar{\sigma}_{xx}(a/2,b/2,h/2)$ | | |
|---|---|---|---|---|---|---|---|---|
| | | | FG | FG-core | | FG | FG-core | |
| | | | | 1-2-2 | 1-1-1 | | 1-2-2 | 1-1-1 |
| 0 | SSDT [39] | | - | 0.5446 | 0.5698 | - | -1.7508 | -1.6663 |
| | TSDT [39] | | - | 0.5446 | 0.5698 | - | -1.7508 | -1.6663 |
| | Present SSDT | | 0.4803 | 0.5446 | 0.5698 | -2.0797 | -1.7508 | -1.6663 |
| | Present TSDT | | 0.4803 | 0.5446 | 0.5698 | -2.0797 | -1.7508 | -1.6663 |
| | Quasi-3D[(a)] (SSDT) [40] | z=h/2 | - | 0.5269 | 0.5526 | - | -1.8544 | -1.7284 |
| | | z=0 | - | 0.5144 | 0.5395 | - | - | - |
| | Present quasi-3D[(a)] (SSDT) | z=h/2 | 0.4616 | 0.5269 | 0.5527 | -2.2871 | -1.8554 | -1.7294 |
| | | z=0 | 0.4502 | 0.5144 | 0.5395 | - | - | - |
| | Present quasi-3D[(a)] (TSDT) | z=h/2 | 0.4591 | 0.5227 | 0.5492 | -1.9369 | -1.4456 | -1.3174 |
| | | z=0 | 0.4480 | 0.5103 | 0.5364 | - | - | - |
| | Present quasi-3D[(b)] (SSDT) | z=h/2 | 0.4945 | 0.5673 | 0.5949 | -2.8019 | -2.0559 | -1.8381 |
| | | z=0 | 0.4823 | 0.5540 | 0.5810 | - | - | - |
| | Present quasi-3D[(b)] (TSDT) | z=h/2 | 0.4897 | 0.5587 | 0.5884 | -2.0592 | -1.1907 | -0.9646 |
| | | z=0 | 0.4779 | 0.5455 | 0.5747 | - | - | - |
| 1 | SSDT [39] | | - | 0.5731 | 0.5788 | - | -1.6745 | -1.6646 |
| | TSDT [39] | | - | 0.5731 | 0.5788 | - | -1.6745 | -1.6645 |
| | Present SSDT | | 0.5798 | 0.5731 | 0.5788 | -1.5220 | -1.6745 | -1.6646 |
| | Present TSDT | | 0.5798 | 0.5731 | 0.5788 | -1.5220 | -1.6745 | -1.6645 |
| | Quasi-3D[(a)] (SSDT) [40] | z=h/2 | - | 0.5561 | 0.5624 | - | -1.7377 | -1.7204 |
| | | z=0 | - | 0.5429 | 0.5490 | - | - | - |
| | Present quasi-3D[(a)] (SSDT) | z=h/2 | 0.5597 | 0.5562 | 0.5624 | -1.5307 | -1.7388 | -1.7215 |
| | | z=0 | 0.5461 | 0.5430 | 0.5491 | | - | - |
| | Present quasi-3D[(a)] (TSDT) | z=h/2 | 0.5571 | 0.5529 | 0.5593 | -1.1158 | -1.3257 | -1.3097 |
| | | z=0 | 0.5439 | 0.5400 | 0.5464 | | - | - |
| | Present quasi-3D[(b)] (SSDT) | z=h/2 | 0.6006 | 0.5987 | 0.6055 | -1.4865 | -1.8563 | -1.8267 |
| | | z=0 | 0.5861 | 0.5847 | 0.5913 | | | |
| | Present quasi-3D[(b)] (TSDT) | z=h/2 | 0.5959 | 0.5926 | 0.5999 | -0.6062 | -0.9800 | -0.9520 |
| | | z=0 | 0.5818 | 0.5789 | 0.5861 | - | - | - |
| 5 | SSDT [39] | | - | 0.5799 | 0.5807 | - | -1.6732 | -1.6638 |
| | TSDT [39] | | - | 0.5799 | 0.5807 | - | -1.6732 | -1.6637 |
| | Present SSDT | | 0.6247 | 0.5799 | 0.5807 | -1.0700 | -1.6732 | -1.6638 |

| | | | | | | | |
|---|---|---|---|---|---|---|---|
| Present TSDT | | 0.6248 | 0.5799 | 0.5807 | -1.0699 | -1.6732 | -1.6637 |
| Quasi-3D[(a)] (SSDT) [40] | z=h/2 | - | 0.5638 | 0.5641 | - | -1.7318 | -1.7156 |
| | z=0 | - | 0.5505 | 0.5507 | - | - | - |
| Present quasi-3D[(a)] (SSDT) | z=h/2 | 0.6004 | 0.5638 | 0.5641 | -0.9094 | -1.7329 | -1.7167 |
| | z=0 | 0.5853 | 0.5505 | 0.5507 | - | - | - |
| Present quasi-3D[(a)] (TSDT) | z=h/2 | 0.5990 | 0.5607 | 0.5611 | -0.4848 | -1.3207 | -1.3067 |
| | z=0 | 0.5847 | 0.5477 | 0.5482 | - | - | - |
| Present quasi-3D[(b)] (SSDT) | z=h/2 | 0.6419 | 0.6073 | 0.6071 | -0.3865 | -1.8475 | -1.8182 |
| | z=0 | 0.6258 | 0.5931 | 0.5929 | - | - | - |
| Present quasi-3D[(b)] (TSDT) | z=h/2 | 0.6398 | 0.6016 | 0.6020 | 0.5162 | -0.9718 | -0.9469 |
| | z=0 | 0.6246 | 0.5878 | 0.5881 | - | - | - |

[(a)]: Results obtained with $\left[Q_{ii}^{2D}, Q_{ij}^{2D}\right]$; [(b)]: Results obtained with $\left[Q_{ii}^{3D}, Q_{ij}^{3D}\right]$

Table 5: Non-dimensional fundamental frequencies $\hat{\omega}$ of $Al/Al_2O_3$ microplates.

| a/h | h/l | Theory | p | | | | |
|---|---|---|---|---|---|---|---|
| | | | 0 | 0.5 | 1 | 5 | 10 |
| 5 | 1 | TSDT [38] | 12.9565 | 11.4813 | 10.5983 | 8.4762 | 7.8468 |
| | | Present TSDT | 13.1645 | 11.6622 | 10.7482 | 8.5714 | 7.9417 |
| | | Quasi-3D (TSDT) [38] | 12.4747 | 11.1097 | 10.2849 | 8.2027 | 7.5480 |
| | | Present quasi-3D (TSDT) | 12.5865 | 11.2082 | 10.3732 | 8.2599 | 7.6030 |
| | 2 | TSDT [38] | 8.1759 | 7.1553 | 6.5542 | 5.3491 | 5.0233 |
| | | Present TSDT | 8.3177 | 7.2634 | 6.6505 | 5.4479 | 5.1267 |
| | | Quasi-3D (TSDT) [38] | 7.7588 | 6.8328 | 6.2857 | 5.1083 | 4.7628 |
| | | Present quasi-3D (TSDT) | 7.8212 | 6.8784 | 6.3301 | 5.1591 | 4.8150 |
| | 4 | TSDT [38] | 6.4393 | 5.5604 | 5.0553 | 4.1718 | 3.9619 |
| | | Present TSDT | 6.5027 | 5.6107 | 5.0984 | 4.2352 | 4.0303 |
| | | Quasi-3D (TSDT) [38] | 6.0161 | 5.2220 | 4.7737 | 3.9453 | 3.7260 |
| | | Present quasi-3D (TSDT) | 6.0397 | 5.2428 | 4.7924 | 3.9796 | 3.7606 |
| | 8 | TSDT [38] | 5.9205 | 5.0878 | 4.6015 | 3.8080 | 3.6331 |
| | | Present TSDT | 5.9413 | 5.1018 | 4.6169 | 3.8310 | 3.6582 |
| | | Quasi-3D (TSDT) [38] | 5.4951 | 4.7406 | 4.3143 | 3.5943 | 3.4113 |
| | | Present quasi-3D (TSDT) | 5.4983 | 4.7429 | 4.3193 | 3.6038 | 3.4226 |
| 10 | 1 | TSDT [38] | 13.6329 | 12.0824 | 11.1415 | 8.9022 | 8.2367 |
| | | Present TSDT | 13.7017 | 12.1439 | 11.1933 | 8.9284 | 8.2615 |
| | | Quasi-3D (TSDT) [38] | 13.2922 | 11.8250 | 10.9199 | 8.7034 | 8.0198 |
| | | Present quasi-3D (TSDT) | 13.3344 | 11.8606 | 10.9617 | 8.7279 | 8.0421 |
| | 2 | TSDT [38] | 8.7651 | 7.6413 | 6.9954 | 5.7361 | 5.3998 |
| | | Present TSDT | 8.8098 | 7.6774 | 7.0202 | 5.7651 | 5.4330 |
| | | Quasi-3D (TSDT) [38] | 8.3187 | 7.3006 | 6.7130 | 5.4839 | 5.1335 |
| | | Present quasi-3D (TSDT) | 8.3415 | 7.3148 | 6.7225 | 5.5062 | 5.1525 |
| | 4 | TSDT [38] | 7.0338 | 6.0428 | 5.4762 | 4.5989 | 4.3928 |
| | | Present TSDT | 7.0538 | 6.0534 | 5.4902 | 4.6190 | 4.4186 |
| | | Quasi-3D (TSDT) [38] | 6.5011 | 5.6087 | 5.1293 | 4.3069 | 4.0903 |
| | | Present quasi-3D (TSDT) | 6.5153 | 5.6282 | 5.1396 | 4.3282 | 4.1092 |
| | 8 | TSDT [38] | 6.5258 | 5.5750 | 5.0315 | 4.2613 | 4.0974 |
| | | Present TSDT | 6.5333 | 5.5692 | 5.0309 | 4.2690 | 4.1078 |
| | | Quasi-3D (TSDT) [38] | 5.9678 | 5.1146 | 4.6442 | 3.9723 | 3.7809 |
| | | Present quasi-3D (TSDT) | 5.9704 | 5.1197 | 4.6597 | 3.9724 | 3.7955 |

Table 6: Non-dimensional fundamental frequencies $\bar{\omega}$ of $Si_3N_4$/SUS304 plates $(\Delta T = 400K \text{ and } a/h = 10)$.

| p | Theory | TID solution | | | TD solution | | |
|---|---|---|---|---|---|---|---|
| | | a/b = 1 | a/b = 2 | a/b = 3 | a/b = 1 | a/b = 2 | a/b = 3 |
| 0 | CPT [41] | 11.417 | 30.671 | 61.696 | 10.512 | 29.123 | 59.048 |
| | FSDT [41] | 11.095 | 29.001 | 56.078 | 10.187 | 27.485 | 53.584 |
| | TSDT [41] | 11.033 | 28.696 | 55.121 | 10.124 | 27.186 | 52.652 |
| | Present TSDT | 11.170 | 28.966 | 55.547 | 10.302 | 27.527 | 53.187 |
| | Present quasi-3D (TSDT) (+) | 11.099 | 28.884 | 55.571 | 10.204 | 27.399 | 53.139 |
| | Present quasi-3D (TSDT) (++) | 10.084 | 28.139 | 55.010 | 8.858 | 26.459 | 52.442 |
| 0.5 | CPT [41] | 7.448 | 20.776 | 42.166 | 6.642 | 19.431 | 39.870 |
| | FSDT [41] | 7.217 | 19.622 | 38.330 | 6.405 | 18.306 | 36.174 |
| | TSDT [41] | 7.174 | 19.417 | 37.694 | 6.362 | 18.108 | 35.563 |
| | Present TSDT | 7.264 | 19.571 | 37.886 | 6.479 | 18.299 | 35.805 |
| | Present quasi-3D (TSDT) (+) | 7.201 | 19.500 | 37.905 | 6.392 | 18.191 | 35.769 |
| | Present quasi-3D (TSDT) (++) | 6.163 | 18.781 | 37.371 | 4.976 | 17.295 | 35.115 |
| 1 | CPT [41] | 6.388 | 18.142 | 37.008 | 5.619 | 16.863 | 34.819 |
| | FSDT [41] | 6.176 | 17.099 | 33.549 | 5.401 | 15.848 | 31.491 |
| | TSDT [41] | 6.135 | 16.909 | 32.959 | 5.359 | 15.662 | 30.923 |
| | Present TSDT | 6.204 | 17.011 | 33.057 | 5.445 | 15.785 | 31.039 |
| | Present quasi-3D (TSDT) (+) | 6.139 | 16.932 | 33.042 | 5.357 | 15.673 | 30.975 |
| | Present quasi-3D (TSDT) (++) | 5.088 | 16.231 | 32.526 | 3.902 | 14.804 | 30.351 |
| 5 | CPT [41] | 4.969 | 14.606 | 30.070 | 4.266 | 13.433 | 28.036 |
| | FSDT [41] | 4.776 | 13.687 | 27.034 | 4.063 | 12.534 | 25.108 |
| | TSDT [41] | 4.732 | 13.491 | 26.437 | 4.015 | 12.336 | 24.514 |
| | Present TSDT | 4.841 | 13.675 | 26.689 | 4.156 | 12.556 | 24.810 |
| | Present quasi-3D (TSDT) (+) | 4.757 | 13.551 | 26.569 | 4.042 | 12.394 | 24.637 |
| | Present quasi-3D (TSDT) (++) | 3.695 | 12.898 | 26.104 | 2.539 | 11.608 | 24.094 |

(+): Exclusion of thermal thickness stress $\left(\sigma_{zz}^T = 0\right)$, (++): Inclusion of thermal thickness stress $\left(\sigma_{zz}^T \neq 0\right)$

Table 7: Non-dimensional critical buckling loads of $Mat_1/Mat_2$ microplates.

| h/l | Theory | $a/h=5$ | | | $a/h=10$ | | | $a/h=20$ | | |
|---|---|---|---|---|---|---|---|---|---|---|
| | | p=0 | 1 | 10 | p=0 | 1 | 10 | 0 | 1 | 10 |
| 1 | RPT [26] | 82.694 | 43.809 | 15.952 | 88.542 | 46.537 | 16.603 | 90.180 | 47.291 | 16.779 |
| | RPT [28] | 78.968 | 42.039 | 15.407 | 87.378 | 45.998 | 16.443 | 89.872 | 47.149 | 16.738 |
| | Present TSDT | 85.767 | 45.262 | 16.272 | 89.332 | 46.908 | 16.605 | 89.047 | 47.027 | 16.319 |
| | Quasi-3D (RPT) [28] | 73.693 | 39.887 | 14.529 | 85.604 | 45.822 | 16.482 | 89.402 | 47.660 | 17.083 |
| | Present quasi-3D (TSDT) | 86.070 | 45.969 | 16.576 | 89.332 | 47.312 | 17.009 | 89.047 | 47.027 | 16.319 |
| 2 | Present TSDT | 33.372 | 16.562 | 6.517 | 35.961 | 17.587 | 6.885 | 36.424 | 17.848 | 6.540 |
| | Present quasi-3D (TSDT) | 34.028 | 17.420 | 6.820 | 36.163 | 18.394 | 7.289 | 36.443 | 18.665 | 7.352 |
| 4 | Present TSDT | 19.952 | 9.321 | 3.841 | 22.535 | 10.212 | 4.353 | 23.070 | 10.545 | 4.484 |
| | Present quasi-3D (TSDT) | 20.937 | 10.280 | 4.194 | 22.939 | 11.020 | 4.757 | 23.474 | 10.949 | 4.888 |
| 8 | Present TSDT | 16.504 | 7.476 | 3.057 | 19.197 | 8.439 | 3.692 | 20.020 | 8.707 | 3.858 |
| | Present quasi-3D (TSDT) | 17.627 | 8.473 | 3.423 | 19.601 | 9.247 | 4.146 | 20.020 | 9.313 | 4.262 |
| Classical | RPT [26] | 15.332 | 6.861 | 2.767 | 18.075 | 7.828 | 3.497 | 18.924 | 8.114 | 3.745 |
| | RPT [28] | 15.332 | 6.861 | 2.770 | 18.076 | 7.828 | 3.498 | 18.924 | 8.114 | 3.745 |
| | Present TSDT | 15.332 | 6.861 | 2.767 | 18.075 | 7.828 | 3.497 | 18.924 | 8.113 | 3.745 |
| | Quasi-3D (RPT) [28] | 15.363 | 7.391 | 3.012 | 18.156 | 8.540 | 3.892 | 18.968 | 8.864 | 4.185 |
| | Present quasi-3D (TSDT) | 16.527 | 7.876 | 3.148 | 18.489 | 8.673 | 3.930 | 19.037 | 8.891 | 4.188 |

Table 8: Critical buckling temperatures $\Delta T_{cr}\left[K\right]$ of $Al/Al_2O_3$ microplates.

| p | h/l | Theory | Uniform temperature | | | Linear temperature | | |
|---|---|---|---|---|---|---|---|---|
| | | | a/h=100 | 20 | 10 | 100 | 20 | 10 |
| 0 | Classical | HSDT [42] | 17.080 | 421.530 | 1618.680 | 24.170 | 833.070 | 3227.360 |
| | | HSDT [43] | 17.089 | 421.540 | 1618.750 | 24.179 | 833.079 | 3227.510 |
| | | CBT [31] | 17.099 | - | - | 24.198 | - | - |
| | | Present TSDT | 17.089 | 421.535 | 1618.689 | 24.177 | 833.073 | 3227.377 |
| | | Present quasi-3D (TSDT) | 17.083 | 423.290 | 1644.410 | 24.182 | 836.576 | 3278.829 |
| | 2 | CBT [31] | 35.053 | - | - | 60.107 | - | - |
| | | Present TSDT | 35.042 | 870.790 | 3419.221 | 60.084 | 1731.582 | 6828.442 |
| | | Present quasi-3D (TSDT) | 35.042 | 871.571 | 3431.200 | 60.086 | 1733.152 | 6852.410 |
| | 1 | CBT [31] | 88.916 | - | - | 167.831 | - | - |
| | | Present TSDT | 88.902 | 2215.320 | 8772.104 | 167.806 | 4420.639 | 17534.209 |
| | | Present quasi-3D (TSDT) | 88.891 | 2215.610 | 8776.800 | 167.798 | 4421.229 | 17543.610 |
| 1 | Classical | HSDT [42] | 7.940 | 196.260 | 758.390 | 5.510 | 358.710 | 1412.960 |
| | | HSDT [43] | 7.940 | 196.267 | 758.424 | 5.513 | 358.715 | 1413.020 |
| | | CBT [31] | 7.944 | - | - | 5.521 | - | - |
| | | Present TSDT | 7.939 | 196.266 | 758.398 | 5.512 | 358.713 | 1412.975 |
| | | Present quasi-3D (TSDT) | 8.174 | 202.797 | 790.829 | 5.955 | 370.963 | 1473.811 |
| | 2 | CBT [31] | 17.852 | - | - | 24.104 | - | - |
| | | Present TSDT | 17.846 | 443.874 | 1747.416 | 24.093 | 823.094 | 3267.841 |
| | | Present quasi-3D (TSDT) | 18.082 | 450.093 | 1775.366 | 24.541 | 834.758 | 3320.262 |
| | 1 | CBT [31] | 47.577 | - | - | 79.852 | - | - |
| | | Present TSDT | 47.571 | 1185.721 | 4699.088 | 79.839 | 2214.401 | 8803.603 |
| | | Present quasi-3D (TSDT) | 47.803 | 1191.776 | 4724.691 | 80.285 | 2225.760 | 8851.616 |
| 5 | Classical | HSDT [42] | 7.260 | 178.530 | 679.310 | 3.891 | 298.700 | 1160.680 |
| | | HSDT [43] | 7.260 | 178.516 | 679.039 | 3.890 | 298.672 | 1160.220 |
| | | CBT [31] | 7.266 | - | - | 3.900 | - | - |
| | | Present TSDT | 7.258 | 178.535 | 679.312 | 3.889 | 298.704 | 1160.689 |
| | | Present quasi-3D (TSDT) | 7.547 | 186.246 | 713.734 | 4.394 | 311.968 | 1219.936 |
| | 2 | CBT [31] | 14.692 | - | - | 16.683 | - | - |
| | | Present TSDT | 14.687 | 365.354 | 1438.925 | 16.674 | 620.276 | 2468.204 |
| | | Present quasi-3D (TSDT) | 14.971 | 372.589 | 1466.682 | 17.181 | 632.736 | 2515.987 |
| | 1 | CBT [31] | 36.971 | - | - | 55.031 | - | - |
| | | Present TSDT | 36.967 | 922.164 | 3663.791 | 55.023 | 1578.709 | 6297.849 |
| | | Present quasi-3D (TSDT) | 37.256 | 929.248 | 3689.120 | 55.530 | 1590.906 | 6341.446 |

Table 9: Non-dimensional deflections of FG and (1-2-2) $Si_3N_4$/SUS304 sandwich microplates under uniform temperature $(a/h=5)$.

| h/l | p | Theory | FG | | FG-core | | Ceramic-core | | **Metal-core** | |
|---|---|---|---|---|---|---|---|---|---|---|
| | | | $\Delta T_1$=300 | 900 | 300 | 900 | 300 | 900 | **300** | **900** |
| 1 | 0 | SSDT | 0 | 0 | -0.381 | -1.075 | 0 | 0 | **0** | **0** |
| | | Quasi-3D (SSDT) | 0 | 0 | -0.435 | -2.713 | 0 | 0 | **0** | **0** |
| | 1 | SSDT | -0.522 | -2.276 | -0.653 | -2.449 | 0.170 | 0.666 | **-0.202** | **-0.920** |
| | | Quasi-3D (SSDT) | -0.585 | -4.523 | -0.696 | -5.036 | 0.159 | 1.094 | **-0.238** | **-2.218** |
| | 5 | SSDT | -0.448 | -2.482 | -0.769 | -3.086 | 0.250 | 0.996 | **-0.238** | **-0.881** |
| | | Quasi-3D (SSDT) | -0.581 | -6.179 | -0.847 | -6.795 | 0.231 | 1.910 | **-0.251** | **-2.021** |
| 5 | 0 | SSDT | 0 | 0 | -1.921 | -5.863 | 0 | 0 | **0** | **0** |
| | | Quasi-3D (SSDT) | 0 | 0 | -2.978 | -17.339 | 0 | 0 | **0** | **0** |
| | 1 | SSDT | -2.437 | -10.724 | -3.171 | -12.921 | 0.862 | 3.658 | **-0.847** | **-3.302** |
| | | Quasi-3D (SSDT) | -3.530 | -23.143 | -4.531 | -28.813 | 1.147 | 7.160 | **-1.286** | **-8.828** |
| | 5 | SSDT | -1.957 | -9.930 | -3.596 | -15.463 | 1.280 | 5.948 | **-1.002** | **-3.296** |
| | | Quasi-3D (SSDT) | -3.057 | -25.040 | -5.167 | -34.746 | 1.685 | 12.749 | **-1.470** | **-8.910** |
| Classical | 0 | SSDT | 0 | 0 | -2.321 | -7.219 | 0 | 0 | **0** | **0** |
| | | Quasi-3D (SSDT) | 0 | 0 | -3.617 | -21.072 | 0 | 0 | **0** | **0** |
| | 1 | SSDT | -2.896 | -12.774 | -3.799 | -15.789 | 1.042 | 4.508 | **-0.985** | **-3.744** |
| | | Quasi-3D (SSDT) | -4.221 | -27.238 | -5.457 | -34.458 | 1.397 | 8.759 | **-1.510** | **-9.975** |
| | 5 | SSDT | -2.296 | -11.478 | -4.274 | -18.685 | 1.551 | 7.490 | **-1.167** | **-3.754** |
| | | Quasi-3D (SSDT) | -3.598 | -28.485 | -6.171 | -40.844 | 2.053 | 15.790 | **-1.737** | **-10.190** |

Table 10: Non-dimensional deflections of FG and (1-2-2) $Si_3N_4$/SUS304 sandwich microplates under linear temperature $(a/h=5)$.

| h/l | p | Theory | FG | | FG-core | | Ceramic-core | | **Metal-core** | |
|---|---|---|---|---|---|---|---|---|---|---|
| | | | $\Delta T_1=0$ | 300 | 0 | 300 | 0 | 300 | 0 | 300 |
| 1 | 0 | SSDT | 0.119 | 0.170 | 0.155 | -0.165 | 0.119 | 0.170 | **0.282** | **0.403** |
| | | Quasi-3D (SSDT) | 0.061 | 0.092 | 0.087 | -0.305 | 0.061 | 0.091 | **0.148** | **0.251** |
| | 1 | SSDT | 0.189 | -0.254 | 0.177 | -0.404 | 0.181 | 0.419 | **0.199** | **0.085** |
| | | Quasi-3D (SSDT) | 0.104 | -0.422 | 0.100 | -0.541 | 0.099 | 0.306 | **0.103** | **-0.071** |
| | 5 | SSDT | 0.237 | -0.108 | 0.189 | -0.502 | 0.211 | 0.537 | **0.158** | **-0.010** |
| | | Quasi-3D (SSDT) | 0.126 | -0.372 | 0.109 | -0.675 | 0.113 | 0.404 | **0.083** | **-0.119** |
| 5 | 0 | SSDT | 0.571 | 0.815 | 0.781 | -0.833 | 0.571 | 0.816 | **1.263** | **1.779** |
| | | Quasi-3D (SSDT) | 0.553 | 0.801 | 0.809 | -1.816 | 0.553 | 0.802 | **1.230** | **1.855** |
| | 1 | SSDT | 0.886 | -1.183 | 0.864 | -1.955 | 0.919 | 2.128 | **0.845** | **0.361** |
| | | Quasi-3D (SSDT) | 0.886 | -2.228 | 0.885 | -3.237 | 0.938 | 2.477 | **0.809** | **-0.074** |
| | 5 | SSDT | 1.042 | -0.476 | 0.888 | -2.336 | 1.085 | 2.761 | **0.677** | **-0.029** |
| | | Quasi-3D (SSDT) | 1.019 | -1.526 | 0.910 | -3.819 | 1.109 | 3.263 | **0.654** | **-0.496** |
| Classical | 0 | SSDT | 0.683 | 0.975 | 0.944 | -1.006 | 0.683 | 0.975 | **1.487** | **2.089** |
| | | Quasi-3D (SSDT) | 0.676 | 0.979 | 0.993 | -2.194 | 0.676 | 0.979 | **1.478** | **2.214** |
| | 1 | SSDT | 1.055 | -1.405 | 1.036 | -2.340 | 1.112 | 2.575 | **0.986** | **0.422** |
| | | Quasi-3D (SSDT) | 1.075 | -2.646 | 1.079 | -3.883 | 1.152 | 3.028 | **0.971** | **-0.065** |
| | 5 | SSDT | 1.224 | -0.560 | 1.058 | -2.774 | 1.316 | 3.347 | **0.792** | **-0.030** |
| | | Quasi-3D (SSDT) | 1.224 | -1.769 | 1.102 | -4.544 | 1.363 | 3.988 | **0.787** | **-0.569** |

Table 11: Non-dimensional fundamental frequencies $\bar{\omega}$ of FG-core $Si_3N_4$/SUS304 microplates under uniform and linear temperatures $(a/h = 10)$.

| Temp. | h/l | $\Delta T_1$ | Theory | 1-2-2 | | | 1-1-1 | | |
|---|---|---|---|---|---|---|---|---|---|
| | | | | 0 | 1 | 5 | 0 | 1 | 5 |
| Uniform | 1 | 300 | TSDT | 22.4338 | 18.6189 | 16.7630 | 19.7294 | 17.1845 | 15.8297 |
| | | | Quasi-3D (TSDT) | 22.0117 | 18.2000 | 16.3504 | 19.3065 | 16.7698 | 15.4215 |
| | | 600 | TSDT | 20.9876 | 17.0665 | 15.1717 | 18.2403 | 15.5951 | 14.2002 |
| | | | Quasi-3D (TSDT) | 20.5158 | 16.5776 | 14.6816 | 17.7495 | 15.1040 | 13.7117 |
| | 2 | 300 | TSDT | 13.5455 | 11.2868 | 10.2184 | 11.9329 | 10.4568 | 9.6866 |
| | | | Quasi-3D (TSDT) | 12.9872 | 10.7364 | 9.6809 | 11.3723 | 9.9151 | 9.1571 |
| | | 600 | TSDT | 11.9747 | 9.7006 | 8.6644 | 10.3869 | 8.8846 | 8.1331 |
| | | | Quasi-3D (TSDT) | 11.2999 | 8.9945 | 7.9589 | 9.6762 | 8.1757 | 7.4303 |
| | 4 | 300 | TSDT | 10.1607 | 8.4986 | 7.7354 | 8.9662 | 7.9025 | 7.3584 |
| | | | Quasi-3D (TSDT) | 9.4653 | 7.8201 | 7.0824 | 8.2688 | 7.2412 | 6.7212 |
| | | 600 | TSDT | 8.2989 | 6.6680 | 5.9843 | 7.1708 | 6.1178 | 5.6288 |
| | | | Quasi-3D (TSDT) | 7.3687 | 5.6853 | 5.0148 | 6.1802 | 5.1373 | 4.6710 |
| | 8 | 300 | TSDT | 9.1121 | 7.6342 | 6.9647 | 8.0472 | 7.1099 | 6.6341 |
| | | | Quasi-3D (TSDT) | 8.3549 | 6.8993 | 6.2634 | 7.2881 | 6.3978 | 5.9539 |
| | | 600 | TSDT | 7.0791 | 5.6485 | 5.0791 | 6.0979 | 5.1835 | 4.7769 |
| | | | Quasi-3D (TSDT) | 5.9950 | 4.4900 | 3.9445 | 4.9322 | 4.0308 | 3.6616 |
| Linear | 1 | 300 | TSDT | 22.4592 | 18.6501 | 16.7943 | 19.7607 | 17.2157 | 15.8591 |
| | | | Quasi-3D (TSDT) | 22.0338 | 18.2277 | 16.3784 | 19.3341 | 16.7976 | 15.4477 |
| | | 600 | TSDT | 21.0472 | 17.1390 | 15.2447 | 18.3125 | 15.6678 | 14.2700 |
| | | | Quasi-3D (TSDT) | 20.5644 | 16.6387 | 14.7433 | 17.8097 | 15.1653 | 13.7704 |
| | 2 | 300 | TSDT | 13.5738 | 11.3207 | 10.2520 | 11.9669 | 10.4904 | 9.7183 |
| | | | Quasi-3D (TSDT) | 13.0113 | 10.7663 | 9.7106 | 11.4020 | 9.9447 | 9.1850 |
| | | 600 | TSDT | 12.0339 | 9.7689 | 8.7311 | 10.4547 | 8.9517 | 8.1975 |
| | | | Quasi-3D (TSDT) | 11.3435 | 9.0473 | 8.0102 | 9.7273 | 8.2272 | 7.4797 |
| | 4 | 300 | TSDT | 10.1934 | 8.5375 | 7.7734 | 9.0051 | 7.9406 | 7.3941 |
| | | | Quasi-3D (TSDT) | 9.4937 | 7.8553 | 7.1168 | 8.3036 | 7.2757 | 6.7535 |
| | | 600 | TSDT | 8.3668 | 6.7443 | 6.0566 | 7.2462 | 6.1911 | 5.6986 |
| | | | Quasi-3D (TSDT) | 7.4182 | 5.7447 | 5.0708 | 6.2367 | 5.1941 | 4.7252 |
| | 8 | 300 | TSDT | 9.1471 | 7.6756 | 7.0049 | 8.0887 | 7.1503 | 6.6718 |
| | | | Quasi-3D (TSDT) | 8.3858 | 6.9374 | 6.3005 | 7.3259 | 6.4350 | 5.9887 |
| | | 600 | TSDT | 7.1531 | 5.7309 | 5.1562 | 6.1793 | 5.2621 | 4.8510 |
| | | | Quasi-3D (TSDT) | 6.0504 | 4.5573 | 4.0072 | 4.9955 | 4.0947 | 3.7225 |

Table 12: Non-dimensional fundamental frequencies $\bar{\omega}$ of ceramic-core $Si_3N_4$/SUS304 microplates under uniform and linear temperatures $(a/h = 10)$.

| Temp. | h/l | $\Delta T_1$ | Theory | 1-2-2 | | | 1-1-1 | | |
|---|---|---|---|---|---|---|---|---|---|
| | | | | 0 | 1 | 5 | 0 | 1 | 5 |
| Uniform | 1 | 300 | TSDT | 28.8114 | 20.2316 | 16.9970 | 28.8114 | 19.5962 | 16.2481 |
| | | | Quasi-3D (TSDT) | 28.3804 | 19.7974 | 16.5421 | 28.3804 | 19.1574 | 15.7836 |
| | | 600 | TSDT | 27.3966 | 18.6788 | 15.3814 | 27.3966 | 18.0212 | 14.5935 |
| | | | Quasi-3D (TSDT) | 26.9733 | 18.1707 | 14.8047 | 26.9733 | 17.4994 | 13.9915 |
| | 2 | 300 | TSDT | 17.5032 | 12.1752 | 10.2190 | 17.5032 | 11.7825 | 9.7630 |
| | | | Quasi-3D (TSDT) | 16.9854 | 11.5797 | 9.5750 | 16.9854 | 11.1744 | 9.0978 |
| | | 600 | TSDT | 15.8513 | 10.5199 | 8.5980 | 15.8513 | 10.1166 | 8.1234 |
| | | | Quasi-3D (TSDT) | 15.3187 | 9.7509 | 7.6754 | 15.3187 | 9.3138 | 7.1393 |
| | 4 | 300 | TSDT | 13.2177 | 9.0990 | 7.6294 | 13.2177 | 8.7970 | 7.2846 |
| | | | Quasi-3D (TSDT) | 12.6045 | 8.3414 | 6.7943 | 12.6045 | 8.0184 | 6.4155 |
| | | 600 | TSDT | 11.2134 | 7.1404 | 5.7616 | 11.2134 | 6.8299 | 5.4041 |
| | | | Quasi-3D (TSDT) | 10.5380 | 6.0225 | 4.3372 | 10.5380 | 5.6433 | 3.8379 |
| | 8 | 300 | TSDT | 11.8927 | 8.1443 | 6.8256 | 11.8927 | 7.8701 | 6.5153 |
| | | | Quasi-3D (TSDT) | 11.2411 | 7.3107 | 5.8976 | 11.2411 | 7.0106 | 5.5456 |
| | | 600 | TSDT | 9.6960 | 5.9987 | 4.7925 | 9.6960 | 5.7144 | 4.4689 |
| | | | Quasi-3D (TSDT) | 8.9467 | 4.6440 | 2.9635 | 8.9467 | 4.2567 | 2.3797 |
| Linear | 1 | 300 | TSDT | 28.8116 | 20.2191 | 16.9825 | 28.8116 | 19.5927 | 16.2436 |
| | | | Quasi-3D (TSDT) | 28.3806 | 19.7860 | 16.5289 | 28.3806 | 19.1542 | 15.7797 |
| | | 600 | TSDT | 27.3956 | 18.6554 | 15.3549 | 27.3956 | 18.0177 | 14.5891 |
| | | | Quasi-3D (TSDT) | 26.9723 | 18.1505 | 14.7823 | 26.9723 | 17.4967 | 13.9887 |
| | 2 | 300 | TSDT | 17.5028 | 12.1621 | 10.2047 | 17.5028 | 11.7792 | 9.7591 |
| | | | Quasi-3D (TSDT) | 16.9849 | 11.5679 | 9.5621 | 16.9849 | 11.1716 | 9.0946 |
| | | 600 | TSDT | 15.8500 | 10.4987 | 8.5764 | 15.8500 | 10.1138 | 8.1199 |
| | | | Quasi-3D (TSDT) | 15.3174 | 9.7342 | 7.6595 | 15.3174 | 9.3121 | 7.1382 |
| | 4 | 300 | TSDT | 13.2169 | 9.0842 | 7.6135 | 13.2169 | 8.7935 | 7.2806 |
| | | | Quasi-3D (TSDT) | 12.6036 | 8.3278 | 6.7797 | 12.6036 | 8.0153 | 6.4122 |
| | | 600 | TSDT | 11.2117 | 7.1170 | 5.7392 | 11.2117 | 6.8270 | 5.4005 |
| | | | Quasi-3D (TSDT) | 10.5363 | 6.0039 | 4.3210 | 10.5363 | 5.6419 | 3.8380 |
| | 8 | 300 | TSDT | 11.8916 | 8.1285 | 6.8088 | 11.8916 | 7.8665 | 6.5112 |
| | | | Quasi-3D (TSDT) | 11.2400 | 7.2959 | 5.8817 | 11.2400 | 7.0073 | 5.5422 |
| | | 600 | TSDT | 9.6941 | 5.9733 | 4.7686 | 9.6941 | 5.7114 | 4.4652 |
| | | | Quasi-3D (TSDT) | 8.9447 | 4.6226 | 2.9440 | 8.9447 | 4.2553 | 2.3807 |

**Table 13: Non-dimensional fundamental frequencies $\bar{\varpi}$ of metal-core $Si_3N_4$/SUS304 microplates under uniform and linear temperatures $(a/h=10)$.**

| Temp. | h/l | $\Delta T_1$ | Theory | 1-2-2 | | | 1-1-1 | | |
|---|---|---|---|---|---|---|---|---|---|
| | | | | 0 | 1 | 5 | 0 | 1 | 5 |
| Uniform | 1 | 300 | TSDT | 11.9407 | 14.9082 | 17.4338 | 11.9407 | 15.2919 | 18.2617 |
| | | | Quasi-3D (TSDT) | 11.4623 | 14.5204 | 17.0666 | 11.4623 | 14.9104 | 17.8979 |
| | | 600 | TSDT | 9.9850 | 13.1901 | 15.8828 | 9.9850 | 13.5931 | 16.7388 |
| | | | Quasi-3D (TSDT) | 9.3046 | 12.7394 | 15.4927 | 9.3046 | 13.1591 | 16.3631 |
| | 2 | 300 | TSDT | 7.3231 | 9.2076 | 10.7613 | 7.3231 | 9.4488 | 11.2728 |
| | | | Quasi-3D (TSDT) | 6.6535 | 8.7145 | 10.3174 | 6.6535 | 8.9689 | 10.8405 |
| | | 600 | TSDT | 5.5929 | 7.6072 | 9.2621 | 5.5929 | 7.8549 | 9.7792 |
| | | | Quasi-3D (TSDT) | 4.4629 | 6.9703 | 8.7523 | 4.4629 | 7.2510 | 9.2999 |
| | 4 | 300 | TSDT | 5.5729 | 7.0523 | 8.2421 | 5.5729 | 7.2399 | 8.6342 |
| | | | Quasi-3D (TSDT) | 4.7358 | 6.4750 | 7.7334 | 4.7358 | 6.6815 | 8.1427 |
| | | 600 | TSDT | 3.7079 | 5.2892 | 6.5676 | 3.7079 | 5.4778 | 6.9544 |
| | | | Quasi-3D (TSDT) | 1.7897 | 4.4490 | 5.9331 | 1.7897 | 4.6918 | 6.3666 |
| | 8 | 300 | TSDT | 5.0284 | 6.3771 | 7.4544 | 5.0284 | 6.5472 | 7.8088 |
| | | | Quasi-3D (TSDT) | 4.1170 | 5.7714 | 6.9264 | 4.1170 | 5.9635 | 7.3006 |
| | | 600 | TSDT | 3.0349 | 4.4826 | 5.6535 | 3.0349 | 4.6516 | 5.9985 |
| | | | Quasi-3D (TSDT) | 0.0000 | 3.5267 | 4.9612 | 0.0000 | 3.7666 | 5.3631 |
| Linear | 1 | 300 | TSDT | 11.9363 | 14.9136 | 17.4425 | 11.9363 | 15.2905 | 18.2615 |
| | | | Quasi-3D (TSDT) | 11.4584 | 14.5251 | 17.0747 | 11.4584 | 14.9091 | 17.8977 |
| | | 600 | TSDT | 9.9800 | 13.2033 | 15.8999 | 9.9800 | 13.5913 | 16.7378 |
| | | | Quasi-3D (TSDT) | 9.3015 | 12.7506 | 15.5082 | 9.3015 | 13.1575 | 16.3622 |
| | 2 | 300 | TSDT | 7.3194 | 9.2132 | 10.7694 | 7.3194 | 9.4475 | 11.2723 |
| | | | Quasi-3D (TSDT) | 6.6504 | 8.7194 | 10.3250 | 6.6504 | 8.9678 | 10.8400 |
| | | 600 | TSDT | 5.5890 | 7.6177 | 9.2730 | 5.5890 | 7.8537 | 9.7782 |
| | | | Quasi-3D (TSDT) | 4.4620 | 6.9779 | 8.7610 | 4.4620 | 7.2500 | 9.2990 |
| | 4 | 300 | TSDT | 5.5694 | 7.0585 | 8.2507 | 5.5694 | 7.2386 | 8.6335 |
| | | | Quasi-3D (TSDT) | 4.7329 | 6.4805 | 7.7416 | 4.7329 | 6.6803 | 8.1420 |
| | | 600 | TSDT | 3.7042 | 5.2992 | 6.5761 | 3.7042 | 5.4767 | 6.9534 |
| | | | Quasi-3D (TSDT) | 1.7910 | 4.4556 | 5.9389 | 1.7910 | 4.6910 | 6.3656 |
| | 8 | 300 | TSDT | 5.0249 | 6.3835 | 7.4633 | 5.0249 | 6.5459 | 7.8080 |
| | | | Quasi-3D (TSDT) | 4.1141 | 5.7773 | 6.9349 | 4.1141 | 5.9622 | 7.2998 |
| | | 600 | TSDT | 3.0312 | 4.4925 | 5.6612 | 3.0312 | 4.6506 | 5.9974 |
| | | | Quasi-3D (TSDT) | 0.0000 | 3.5333 | 4.9659 | 0.0000 | 3.7659 | 5.3620 |

Table 14: Critical buckling temperatures $\Delta T_{cr}\left[K\right]$ of (1-2-2) $Si_3N_4$/SUS304 microplates $\left(a/h=20\right)$.

| Temp. pattern | h/l | Theory | FG core | | | Ceramic core | | | **Metal core** | | |
|---|---|---|---|---|---|---|---|---|---|---|---|
| | | | p=0.2 | 1 | 5 | 0.2 | 1 | 5 | **0.2** | **1** | **5** |
| Uniform | 1 | TSDT | 1053.28 | 1005.92 | 997.92 | 1095.52 | 1018.72 | 979.36 | **724.78** | **835.04** | **977.28** |
| | | Quasi-3D (TSDT) | 1075.20 | 1033.60 | 1052.80 | 1096.96 | 1020.80 | 982.56 | **725.76** | **836.32** | **978.56** |
| | 2 | TSDT | 512.80 | 481.76 | 462.56 | 568.48 | 497.12 | 448.48 | **364.96** | **422.56** | **483.36** |
| | | Quasi-3D (TSDT) | 515.20 | 486.40 | 467.20 | 569.60 | 498.08 | 449.60 | **365.28** | **423.20** | **484.16** |
| | 4 | TSDT | 336.80 | 316.00 | 304.16 | 380.64 | 322.40 | 284.64 | **244.32** | **288.48** | **332.32** |
| | | Quasi-3D (TSDT) | 339.20 | 320.00 | 307.20 | 381.92 | 323.52 | 285.92 | **244.96** | **289.44** | **333.28** |
| | 8 | TSDT | 287.20 | 269.60 | 260.64 | 327.20 | 273.12 | 239.20 | **211.04** | **251.68** | **290.40** |
| | | Quasi-3D (TSDT) | 291.20 | 272.00 | 262.40 | 328.64 | 274.40 | 240.48 | **212.00** | **252.64** | **291.68** |
| | Classical | TSDT | 270.24 | 253.92 | 245.60 | 308.64 | 256.16 | 223.52 | **199.52** | **238.88** | **276.00** |
| | | Quasi-3D (TSDT) | 272.00 | 256.00 | 249.60 | 310.08 | 257.44 | 224.80 | **200.64** | **240.00** | **277.44** |
| Linear | 1 | TSDT | 1041.76 | 993.76 | 980.64 | 1095.84 | 1021.60 | 986.08 | **724.84** | **833.12** | **969.82** |
| | | Quasi-3D (TSDT) | 1064.00 | 1018.72 | 1020.96 | 1097.44 | 1024.00 | 989.76 | **725.44** | **834.08** | **970.88** |
| | 2 | TSDT | 515.36 | 484.64 | 465.44 | 567.84 | 496.48 | 448.16 | **364.96** | **422.88** | **483.36** |
| | | Quasi-3D (TSDT) | 520.00 | 489.60 | 470.72 | 568.80 | 497.44 | 449.12 | **365.44** | **423.36** | **484.16** |
| | 4 | TSDT | 340.32 | 319.84 | 308.00 | 379.68 | 321.12 | 283.68 | **244.32** | **289.12** | **332.96** |
| | | Quasi-3D (TSDT) | 344.16 | 324.00 | 312.48 | 380.96 | 322.24 | 284.64 | **244.96** | **289.92** | **333.92** |
| | 8 | TSDT | 291.04 | 273.76 | 264.48 | 326.24 | 271.84 | 237.92 | **211.04** | **252.00** | **291.36** |
| | | Quasi-3D (TSDT) | 294.88 | 277.92 | 268.96 | 327.52 | 273.12 | 239.04 | **212.00** | **253.12** | **292.48** |
| | Classical | TSDT | 273.76 | 257.76 | 249.44 | 307.68 | 254.88 | 222.24 | **199.84** | **239.52** | **276.96** |
| | | Quasi-3D (TSDT) | 277.92 | 262.08 | 254.08 | 309.12 | 256.00 | 223.36 | **200.64** | **240.64** | **278.24** |